CARD8 inflammasome activation during HIV-1 cell-to-cell transmission

Jessie Kulsuptrakul[1,2], Michael Emerman[2,*], Patrick S. Mitchell[3,4*]
[1]Molecular and Cellular Biology Graduate Program, University of Washington, Seattle, WA 98195, USA

[2]Divisions of Human Biology and Basic Sciences, Fred Hutchinson Cancer Center, Seattle, WA 98109, USA

[3]Department of Microbiology, University of Washington, Seattle, WA 98109, USA

[4]Howard Hughes Medical Institute, University of Washington, Seattle, WA, 98109, USA

***Corresponding authors:** memerman@fredhutch.org, psmitche@uw.edu

Abstract

Our previous work demonstrated that CARD8 detects HIV-1 infection by sensing the enzymatic activity of the HIV protease, resulting in CARD8-dependent inflammasome activation (Kulsuptrakul et al., 2023). CARD8 harbors a motif in its N-terminus that functions as a HIV protease substrate mimic, permitting innate immune recognition of HIV-1 protease activity, which when cleaved by HIV protease triggers CARD8 inflammasome activation. Here, we sought to understand CARD8 responses in the context of HIV-1 cell-to-cell transmission via a viral synapse. We observed that cell-to-cell transmission of HIV-1 between infected T cells and primary human monocyte-derived macrophages induces CARD8 inflammasome activation in a manner that is dependent on viral protease activity and largely independent of the NLRP3 inflammasome. Additionally, to further evaluate the viral determinants of CARD8 sensing, we tested a panel of HIV protease inhibitor resistant clones to establish how variation in HIV protease affects CARD8 activation. We identified mutant HIV-1 proteases that differentially cleave and activate CARD8 compared to wildtype HIV-1, thus indicating that natural variation in HIV protease affects not only the cleavage of the viral Gag-Pol polyprotein but also likely impacts innate sensing and inflammation.

33 **INTRODUCTION**

34 HIV-1 disease progression is characterized by chronic inflammation, immune activation,
35 CD4+ T cell depletion and eventual destruction of the immune system and susceptibility to
36 opportunistic infections. The primary cellular targets of HIV-1 are activated CD4+ T helper cells,
37 specialized CD4+ T cell subtypes such as Th17 cells (Brenchley et al., 2008; Gosselin et al.,
38 2009; Rodriguez-Garcia et al., 2014), central memory cells (Chun et al., 1997b, 1997a, 1995),
39 and macrophages (Collman et al., 1990, 1989). Chronic immune activation is primarily caused
40 by rapid depletion of mucosal Th17 cells responsible for maintaining gut epithelial barrier
41 integrity (Brenchley et al., 2008, 2006). In addition to inflammation induced by circulating
42 microbial ligands, inflammation can also originate from HIV-infected cells through activation of
43 innate immune sensors that form cytosolic immune complexes known as inflammasomes.
44 Inflammasome activation ultimately results in activation of pro-inflammatory caspases including
45 caspase 1 (CASP1). Active CASP1 processes inflammatory cytokines and activates the pore-
46 forming protein gasdermin D (GSDMD), which forms small pores in the plasma membrane and
47 initiates a lytic form of cell death known as pyroptosis and the release of mature inflammatory
48 cytokines interleukin (IL)-1β and IL-18 (Broz and Dixit, 2016; Fink and Cookson, 2005).

49 In prior work, we and others showed that the inflammasome-forming sensor CARD8
50 senses HIV-1 infection through the detection of HIV-1 protease (HIV^{PR}) activity (Clark et al.,
51 2022; Kulsuptrakul et al., 2023; Wang et al., 2021). While the canonical function of HIV^{PR} is to
52 cleave viral polyproteins during virion maturation, active HIV^{PR} is also released into the host cell,
53 which is sensed by CARD8 via HIV^{PR} cleavage of its N-terminus and subsequent inflammasome
54 activation. In this way, the CARD8 N-terminus functions as a “molecular tripwire” to recognize
55 the enzymatic activity of HIV^{PR} and other viral proteases (Castro and Daugherty, 2023; Nadkarni
56 et al., 2022; Tsu et al., 2023). Moreover, HIV^{PR} cleavage of CARD8 occurs rapidly after infection
57 such that HIV^{PR} inhibitors and fusion inhibitors, but not reverse transcriptase (RT) inhibitors can
58 prevent CARD8 inflammasome activation, implying that CARD8 detects HIV-1 viral protease

59 activity of virion-packaged or “incoming” HIV^{PR} upon virion fusion (Kulsuptrakul et al., 2023;
60 Wang et al., 2024, 2021). Interestingly, CARD8 inflammasome activation in resting CD4+ T cells
61 results in pyroptosis but not the release of pro-inflammatory cytokines IL-1β or IL-18 (Wang et
62 al., 2024), suggesting that CARD8 inflammasome activation in T cells does not directly
63 contribute to chronic inflammation. Here, we address whether or not CARD8 may influence HIV-
64 1 pathogenesis through the maturation and release of IL-1β from infected macrophages.

65 HIV-1 can be transmitted from one cell to another via two main mechanisms: “cell-free”
66 infection through binding of free HIV-1 virions to target cells, and cell-to-cell infection whereby
67 infected cells directly transfer virus to an uninfected target cell via the formation of a transient
68 viral synapse (Chen et al., 2007; Galloway et al., 2015; Iwami et al., 2015). Cell-to-cell
69 transmission of HIV-1 has been reported between multiple HIV-1 target cell types including
70 between active and resting CD4+ T cells (Agosto et al., 2018; Martin et al., 2010) and between
71 CD4+ T cells and macrophages (Baxter et al., 2014; Dupont and Sattentau, 2020; Lopez et al.,
72 2019). Cell-to-cell transmission delivers a large influx of virus to target cells, resulting in a high
73 multiplicity of infection (MOI) (Agosto et al., 2015; Del Portillo et al., 2011; Duncan et al., 2013;
74 Russell et al., 2013), which has been proposed to enhance viral fitness by overwhelming host
75 restriction factors including Tetherin/BST-2 (Jolly et al., 2010; Zhong et al., 2013), SAMHD1 (Xie
76 et al., 2019), and TRIM5α (Richardson et al., 2008), and evading adaptive immune responses
77 including broadly neutralizing antibodies (Abela et al., 2012; Dufloo et al., 2018). Cell-to-cell
78 spread of HIV-1 is thus an important consideration in studying CARD8 inflammasome activation.

79 Here, we investigated both host and viral determinants of CARD8 inflammasome
80 activation upon HIV-1 infection. We evaluated CARD8 sensing of HIV^{PR} during cell-to-cell
81 transmission of HIV-1 from T cell lines to myeloid cells in both immortalized and primary cell
82 models of infection. We found that CARD8 inflammasome activation occurs in the context of
83 cell-to-cell transmission from both SUPT1 cells, a T cell lymphoma cell line, to THP-1 cells, an
84 acute myeloid leukemia cell line, and from primary CD4+ T cells to primary monocyte-derived

85 macrophages. We also observed that HIV-triggered CARD8 inflammasome activation is largely
86 independent of the NLRP3 inflammasome, which has previously been implicated in innate
87 sensing of HIV-1 (Bandera et al., 2018; Chivero et al., 2017; Hernandez et al., 2013; Leal et al.,
88 2020; Mamik et al., 2017; Zhang et al., 2021). Our findings suggest that CARD8 sensing of
89 HIV^{PR} activity during cell-to-cell transmission of HIV-1 to macrophages, leading to robust
90 secretion of IL-1β, may be a source of inflammatory cytokines that promote pathogenic chronic
91 inflammation and disease progression. In addition, we also show that natural variation in HIV^{PR}
92 due to resistance to protease inhibitors also affects CARD8 cleavage and subsequent
93 inflammasome activation. Our results extend the role of incoming HIV^{PR} on CARD8-dependent
94 inflammasome activation of inflammasome responses as a function of cell type, mode of
95 transmission, and virus evolution in response to antiviral therapy.
96
97 **RESULTS**

98 ***Cell-to-cell transmission of HIV-1 induces CARD8 inflammasome activation***

99 Our previous work investigating HIV-dependent CARD8 inflammasome activation used
100 the cationic polymer DEAE-dextran, which is a common reagent used to enhance viral infection
101 in cell culture (Bailey et al., 1984). However, we found that DEAE-dextran could induce
102 inflammasome activation in the absence of viral infection in some “wildtype” (WT) THP-1 cell
103 stocks (see **Supplemental Note**). These results prompted us to establish other models of HIV-1
104 infection and subsequent inflammasome activation that lack cationic polymers. Thus, we
105 designed an *in vitro* coculture infection system to mimic HIV-1 cell-to-cell transmission by
106 infecting SUPT1 cells, a T-cell lymphoma line (i.e., donor cells) and then mixing them with
107 uninfected THP-1 cells (i.e., target cells). We opted for SUPT1 cells as the viral producer cell
108 line because they are permissive to HIV-1 infection, and unlike THP-1 cells, SUPT1 cells do not
109 respond to a known CARD8 inflammasome activator, ValboroPro (VbP), as assayed by both IL-
110 1β secretion and cell death, indicating that SUPT1 cells do not have a functional CARD8

111 inflammasome pathway (**Figure 1A**). This allowed us to infer that inflammasome outputs (e.g.

112 IL-1β secretion) in our coculture system occur upon cell-to-cell transmission of HIV-1 from

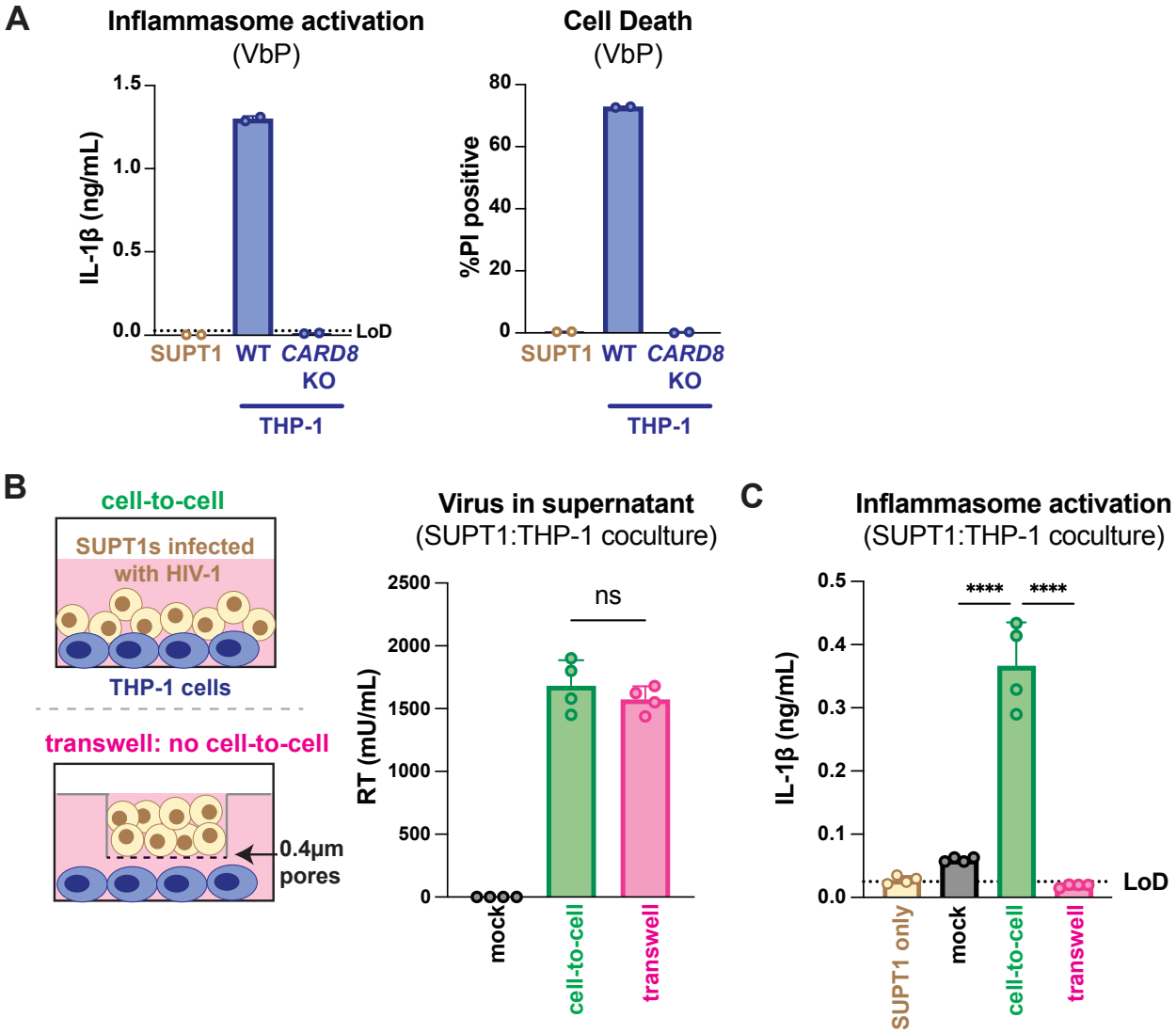

Figure 1. HIV-1 cell-to-cell infection induces inflammasome activation. (**A**) SUPT1 or THP-1 cells were primed with Pam3CSK4 (500ng/mL) overnight then treated with 5µM ValboroPro (VbP) for 24 hours then assessed for IL-1β secretion and cell death via propidium iodide (PI) uptake. %PI positive was normalized to mock control. (**B**) (left) Schematic illustrating experimental setup for SUPT1:THP-1 cell coculture either with (bottom) or without (top) a transwell. (right) SUPT1 cell were either mock infected or infected with HIV-1_{LAI} then cocultured with primed WT THP-1 cells 20 hours post infection. Mock- or HIV-1_{LAI}-infected SUPT1 cells were either mixed with the THP-1 cells or put in a transwell with a virus-permeable membrane as shown in panel B (left). Supernatant in the cell-to-cell condition and in the supernatant outside of the transwell were sampled and measured for infectious HIV virions via reverse transcriptase (RT) assay or (**C**) IL-1β secretion 3 days after starting the coculture. Dotted line indicates limit of detection (LoD). Datasets represent mean ± SD (A: n=2; B,C n=4 biological replicates). One-way ANOVA with (B) Tukey's or (C) Dunnett's test using GraphPad Prism 10. ns = not significant, *p<0.05,**p<0.01, ***p<0.001, ****p<0.0001.

113 SUPT1 cells to the CARD8-competent THP-1 cells.

114 We found that coculture of THP-1 cells with HIV-1_{LAI}-infected SUPT1 cells (**Figure 1B**)
115 but not mock-infected SUPT1 cells results in robust inflammasome activation as indicated by IL-
116 1β secretion, suggesting that our coculture system, which lacks DEAE-dextran, can induce HIV-
117 dependent inflammasome activation via cell-to-cell infection (**Figure 1C**). To further test this
118 assumption, we prevented cell-to-cell contact using a virus-permeable transwell with a 0.4μm
119 pore insert (**Figure 1B,** left). We verified that there were equivalent amounts of infectious virus
120 in the cell-to-cell condition versus the lower chamber of the transwell condition by measuring RT
121 activity in the supernatant (**Figure 1B,** right). Despite equivalent amounts of infectious virus in
122 both conditions, we observed that HIV-1_{LAI}-infected SUPT1 cells (upper chamber) cocultured
123 with THP-1 cells (lower chamber) did not lead to detectable IL-1β secretion (**Figure 1C**). These
124 data suggest that our SUPT1:THP-1 coculture system can trigger HIV-dependent
125 inflammasome activation in a manner dependent on cell-to-cell contact.

126 We next assessed the role of CARD8 and other inflammasome sensors during cell-to-
127 cell transmission of HIV-1. We cocultured mock- or HIV-1_{LAI}-infected SUPT1 cells with either WT
128 or *CARD8* KO THP-1 cells and compared inflammasome activation by measuring levels of
129 secreted IL-1β. HIV-1_{LAI}-infected SUPT1 cells cocultured with WT but not *CARD8* KO THP-1
130 cells resulted in a significant increase in IL-1β (**Figure 2A**). These results suggest that CARD8
131 is the primary sensor that drives inflammasome activation in HIV-1 cell-to-cell transmission to
132 THP-1 cells. Since the NLRP3 inflammasome has previously been implicated in HIV-dependent
133 inflammasome activation (Bandera et al., 2018; Chivero et al., 2017; Hernandez et al., 2013;
134 Leal et al., 2020; Mamik et al., 2017; Zhang et al., 2021), we also assessed the effects of the
135 NLRP3 inflammasome-specific inhibitor MCC950 (Coll et al., 2015; Primiano et al., 2016) on
136 inflammasome activation in our coculture system. Treatment with MCC950 or the caspase 1
137 (CASP1) inhibitor VX765 (Wannamaker et al., 2007) were sufficient to abrogate inflammasome

activation induced by the ionophore nigericin, a well-characterized NLRP3 agonist (**Figure 2– figure supplement 1A**). However, in the HIV-1 coculture system, MCC950 treatment had only a modest effect on inflammasome activation while VX765 and the HIV^{PR} inhibitor lopinavir (LPV), which prevents CARD8 cleavage by HIV-1^{PR} (Kulsuptrakul et al., 2023; Wang et al., 2021), completely abrogated IL-1β secretion (**Figure 2B**). We observed similar results during HIV-1$_{LAI}$ and HIV-1$_{LAI\text{-}VSVG}$ cell-free infection of THP-1 cells in the presence of DEAE-dextran (**Figure 2– figure supplement 1B**). Taken together, these findings indicate that HIV-dependent

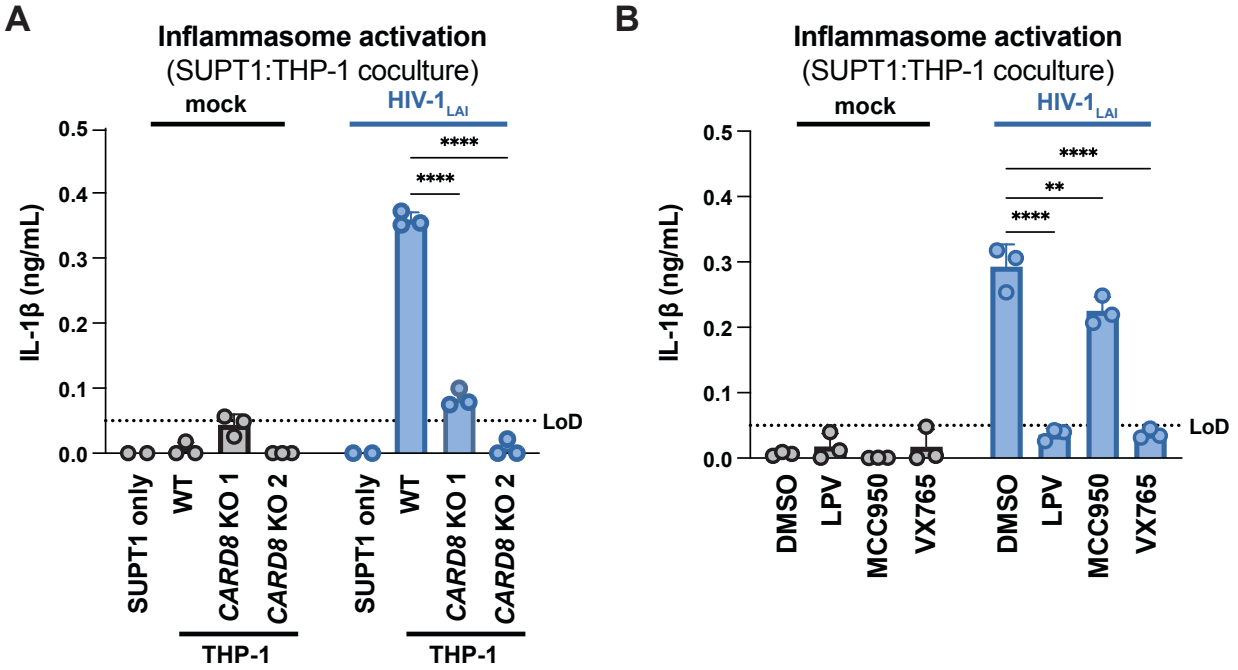

Figure 2. HIV-1 cell-to-cell transmission induces CARD8-dependent activation largely independent of NLRP3. (**A**) SUPT1 cells were either mock-infected or infected with HIV-1$_{LAI}$ for 18-20 hours prior to coculture with wildtype (WT) or *CARD8* knockout (KO) THP-1 cells. The coculture was harvested 72 hours later to probe for IL-1β secretion in the coculture supernatant via IL-1R reporter assay. THP-1 cells were primed with Pam3CSK4 (500ng/mL) for 16-24 hours prior to coculture. SUPT1 cells were infected with HIV-1$_{LAI}$ such that 30% of the cells were positive for intracellular p24^{gag} after 18-20 hours. (**B**) SUPT1 cells were either mock or HIV-1$_{LAI}$-infected as in (A) for 18-20 hours then incubated in DMSO, lopinavir (LPV), MCC950, or VX765 at 0.01%, 5μM, 10μM, or 1μg/mL, respectively, for 15 minutes prior to coculturing with primed WT THP-1 cells. The coculture was assessed for subsequent inflammasome activation after 72 hours as in (A). Dotted line indicates limit of detection (LoD). Datasets represent mean ± SD (n=3 biological replicates). Two-way ANOVA with Dunnett's test using GraphPad Prism 10. ns = not significant, *p<0.05,**p<0.01, ***p<0.001, ****p<0.0001.

145 inflammasome activation via cell-to-cell transmission is CARD8-dependent and largely NLRP3-

146 independent.

147

148

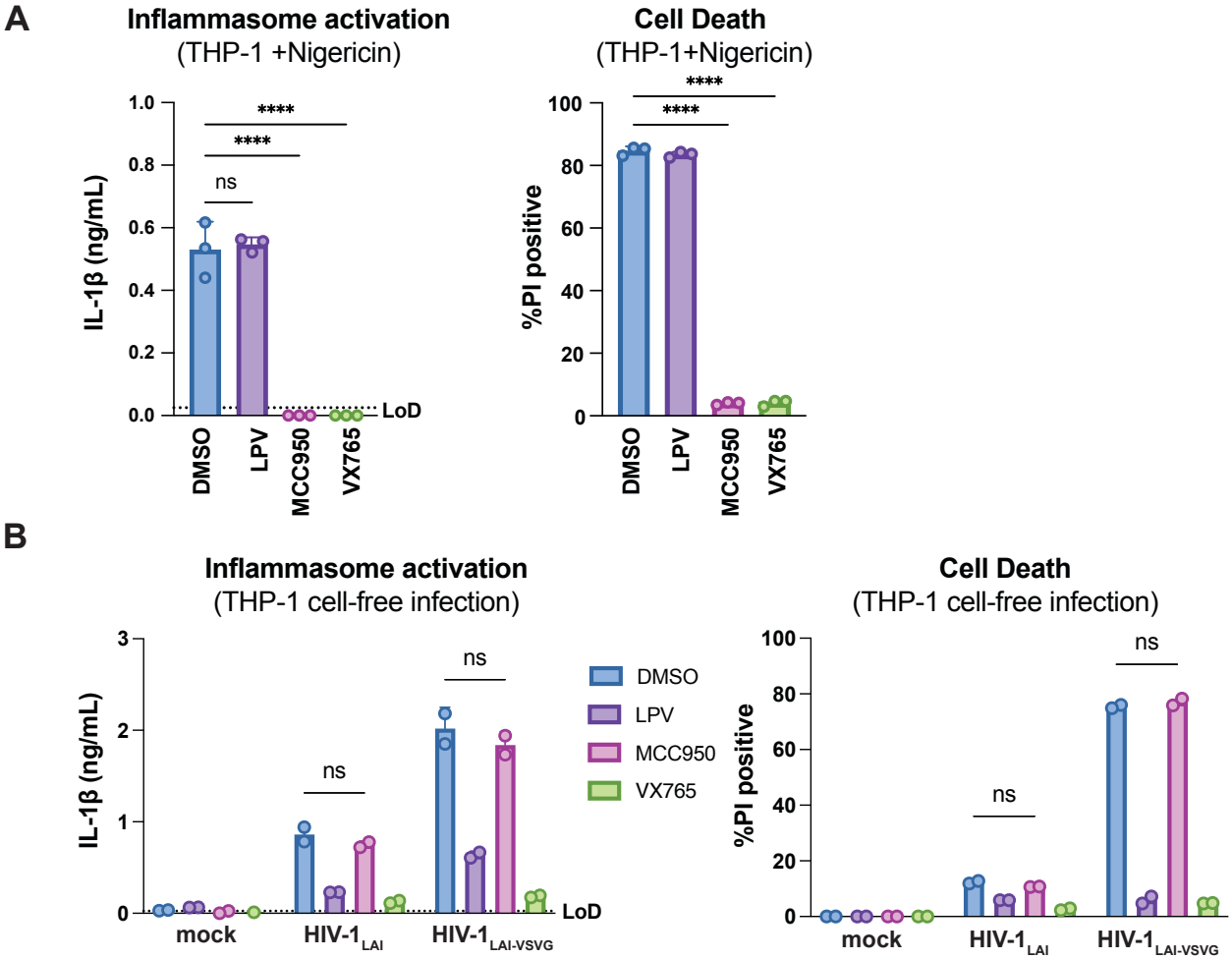

Figure 2– figure supplement 1. HIV-dependent inflammasome activation is largely NLRP3-independent. (**A**) Wildtype THP-1 cells were pre-treated with either DMSO, lopinavir (LPV), MCC950, or VX765 at 0.01%, 5μM, 10μM, or 1μg/mL, respectively, for 15 minutes prior to 4-hour treatment with 5μg/mL nigericin. Subsequent inflammasome activation was assessed via (A, left) IL-1β secretion via IL-1R reporter assay and (A, right) cell death via propidium iodide (PI) dye uptake. (**B**) Wildtype THP-1 cells were pre-treated with indicated inhibitors as in (A) then infected with either HIV-1_{LAI} or VSV-G pseudotyped HIV-1_{LAI} (HIV-$1_{LAI\text{-}VSVG}$) in the presence of 10μg/mL DEAE-dextran such that both HIV-1_{LAI}-infected and HIV-$1_{LAI\text{-}VSVG}$ -infected cells were ~30% positive for intracellular $p24^{gag}$ after 24 hours by flow cytometry. Subsequent inflammasome activation was assessed 24 hours post infection via IL-1β secretion and cell death as in (A). Dotted line indicates limit of detection (LoD). Datasets represent mean ± SD (A: n=3, B: n=2 biological replicates). One-way (A) or Two-way (B) ANOVA with Dunnett's test using GraphPad Prism 10. ns = not significant, *p<0.05,**p<0.01, ***p<0.001, ****p<0.0001.

149 **CARD8, but not NLRP3, is required for inflammasome activation during HIV-1 cell-to-cell**
150 **transmission into primary monocyte-derived macrophages**

151 We next examined inflammasome activation upon HIV-1 cell-to-cell transmission in
152 primary human monocyte-derived macrophages (MDMs). Previously, we had observed that
153 CARD8 could sense active HIV-1^{PR} released into the host cytosol following viral fusion, which
154 we refer to as "incoming" HIV-1^{PR} in our cell-free infection system in THP-1 cells using DEAE-
155 dextran and spinoculation (Kulsuptrakul et al., 2023). Thus, we assessed the importance of viral
156 entry by coculturing MDMs from three independent donors with mock-, HIV-1_{LAI}-, or HIV-$1_{NL4.3-}$
157 $_{BaL}$-infected SUPT1 cells expressing CCR5 (SUPT1-CCR5) and assayed for inflammasome
158 activation (**Figure 3A**). HIV-1_{LAI} is a CXCR4 tropic strain unable to infect macrophages whereas
159 HIV-$1_{NL4.3-BaL}$ uses CCR5 as a co-receptor which is a requirement for infection of macrophages.
160 We observed inflammasome activation, as measured by IL-1β secretion, in MDMs cocultured
161 with HIV-$1_{NL4.3-BaL}$-infected SUPT1 cells but not in MDMs cocultured with mock- or HIV-1_{LAI}-
162 infected SUPT1-CCR5 cells (**Figure 3A**). This demonstrates that HIV-dependent inflammasome
163 activation can occur in MDMs during cell-to-cell infection in a manner dependent on viral entry.
164 To further ascertain if this inflammasome activation was CARD8-dependent and driven by
165 incoming HIV^{PR} during SUPT1:MDM cell-to-cell transmission, we investigated the effects of
166 different inhibitors on inflammasome activation in MDM cocultures with HIV-$1_{NL4.3-BaL}$-infected
167 SUPT1s. We observed that IL-1β secretion was abrogated by treatment with lopinavir, an HIV-1
168 protease inhibitor, and VX765, a CASP1 inhibitor, indicating that inflammasome activation in
169 MDM cocultures is dependent on HIV^{PR} and CASP1, respectively (**Figure 3A**). In addition, we
170 used an RT inhibitor, nevirapine (NVP), to prevent synthesis of *de novo* translated HIV^{PR}, and
171 thus any CARD8-dependent IL-1β secretion would only be due to incoming HIV^{PR} in the
172 presence of NVP. Indeed, we observed HIV-dependent inflammasome activation in the
173 presence of NVP that was added at the time of coculture, indicating that incoming HIV^{PR} is
174 sufficient to elicit an inflammasome response (**Figure 3A**). Lastly, MDM cocultures treated with

175 MCC950, an inhibitor of the NLRP3 inflammasome, had no effect on IL-1β secretion (**Figure**
176 **3A**), and we observed similar inflammasome activation results regardless of whether the MDMs
177 were primed with TLR1/2 agonist Pam3CSK4 versus TLR4 agonist lipopolysaccharide (LPS)
178 (**Figure 3– figure supplement 1A**). Thus, cell-to-cell contact of infected cells with primary
179 monocyte-derived macrophages can elicit an inflammasome response in a manner that is
180 dependent on viral entry, CASP1, and incoming HIV^{PR}, and independent from NLRP3.
181 To further assess the timing of this inflammasome activation, we conducted a
182 SUPT1:MDM time course coculture experiment with 3 additional donors, assaying IL-1β
183 secretion at 4, 24, 48, and 72 hours post coculture in the presence and absence of NVP. We
184 observed inflammasome activation as determined by IL-1β secretion by 24 hours post coculture
185 in all donors that persisted at a similar level at 48 and 72 hours post coculture (**Figure 3B**). As
186 expected, we observed donor-to-donor variation in the extent to which IL-1β secretion occurred
187 following HIV-1 infection. However, per donor, HIV-1-driven IL-1β levels were comparable to
188 that of VbP-induced inflammasome activation (**Figure 3–figure supplement 1B**). Moreover,
189 adding NVP had no effect on IL-1β secretion in HIV-1 infected MDM cocultures (**Figure 3B**). To
190 verify that NVP was functional, we assayed the supernatant of the mock and NVP-treated
191 cocultures from **Figure 3B** at 48 hours post-coculture for infectious virions via an assay for RT
192 activity and observed lower RT activity in NVP-treated MDM donors (**Figure 3–figure**
193 **supplement 1C)**. Unlike the 'cell-free' infection conditions in which we previously observed an
194 increase in IL-1β levels 4h post-infection, we did not detect measurable differences in IL-1β
195 secretion at this early timepoint following the establishment of SUPT1:MDM coculture.
196 Nevertheless, the data are consistent with incoming HIV^{PR} being responsible for inflammasome
197 activation during cell-to-cell transmission of HIV because the induction of IL-1β persists in the
198 presence of NVP which would block any *de novo* synthesis of new *gag/pol* products (**Figure 3A**
199 **and B**). Taken together, these data suggest that in the context of cell-to-cell transmission,

200 CARD8 is likely the inflammasome-forming sensor that detects HIV-1 infection via incoming
201 HIV^{PR} activity in primary monocyte-derived macrophages.
202 To specifically address the role of CARD8 in HIV-1 induced inflammasome activation in
203 MDMs, we genetically edited MDMs by isolating monocytes from five donors and
204 electroporating them with Cas9 RNPs complexed with three unique sgRNAs per gene targeting
205 *AAVS1*, a safe harbor locus, *CARD8* or *NLRP3* (only 2 donors for *NLRP3* KO). Edited MDMs
206 were then differentiated for 6 days prior to evaluating KO efficiency and initiating cocultures with
207 HIV-1-infected SUPT1 cells. To verify KO efficiency, we immunoblotted with an antibody that
208 detects the CARD8 C-terminus in *CARD8* KO MDMs relative to the *AAVS1* KO control and
209 observed a marked reduction of the full-length and FIIND-processed CARD8 protein in all 5
210 donors (**Figure 3C**). In addition, we confirmed *AAVS1*, *CARD8*, and *NLRP3* KO at the genetic
211 level via Synthego ICE analysis (Conant et al., 2022), measuring >85% KO efficiency (**Figure**
212 **3C**). We also observed robust inflammasome activation upon treatment with CARD8
213 inflammasome activator VbP as measured by IL-1β secretion in *AAVS1* KO MDMs from 2 of the
214 3 donors, which was completely abrogated in *CARD8* KO MDMs, confirming functional loss of
215 CARD8 (**Figure 3– figure supplement 1D**). We then cocultured either *AAVS1* KO, *CARD8* KO,
216 or *NLRP3* KO MDMs with mock or HIV-$1_{NL4.3\text{-}BaL}$-infected SUPT1-CCR5 cells at a 1:1 ratio and
217 measured inflammasome activation via IL-1β secretion 48 hours post-coculture. In all 5 donors,
218 we observed significant reduction in inflammasome activation in *CARD8* KO cocultures relative
219 to the *AAVS1* KO control (**Figure 3D**). Consistent with our findings with SUPT1:THP-1
220 coculture, we observed no difference in inflammasome activation when coculturing infected
221 SUPT1 cells with *AAVS1* KO vs *NLRP3* KO MDMs, suggesting that the inflammasome
222 activation was also largely NLRP3-independent (**Figure 3D**). Taken together, these data
223 demonstrate that CARD8 is required for inflammasome activation in MDMs during HIV-1 cell-to
224 cell transmission.

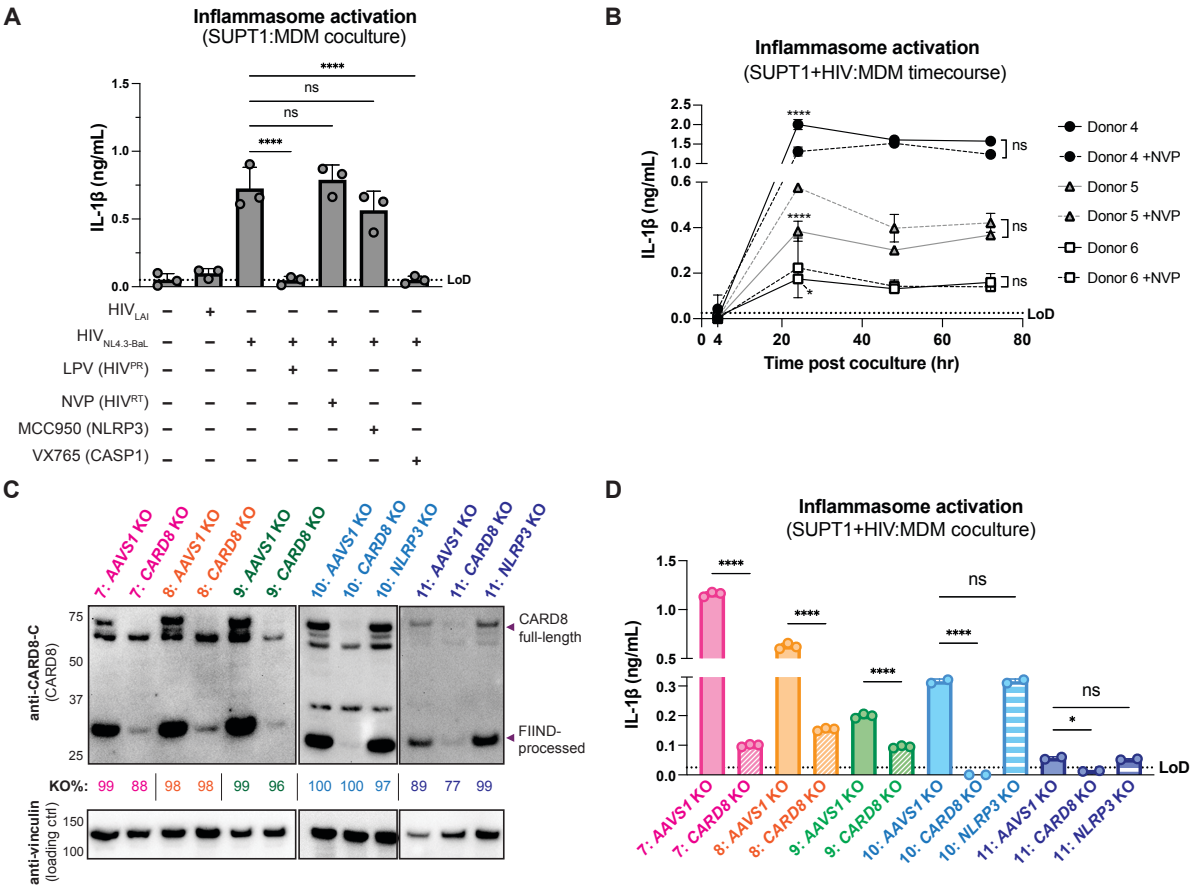

Figure 3. Cell-to-cell HIV infection induces CARD8-dependent inflammasome activation in monocyte-derived macrophages (MDMs). (**A**) MDMs from 3 independent donors were cocultured with SUPT1 cells expressing CCR5 (SUPT1-CCR5) that were mock-, HIV-1_{LAI}- or HIV-$1_{NL4.3\text{-}BaL}$-infected then assayed for inflammasome activation 48 hours post-coculture for IL-1β secretion. Fifteen minutes before starting the coculture, SUPT1-CCR5 cells infected with HIV-$1_{NL4.3\text{-}BaL}$ were pre-treated with either DMSO, lopinavir (5μM), nevirapine (50μM), MCC950 (10μM) or VX765 (1μg/mL), inhibiting HIV-1 protease (HIV^{PR}), HIV-1 reverse transcriptase (HIV^{RT}), NLRP3, or caspase 1 (CASP1), respectively. (**B)** MDMs from 3 independent donors were cocultured with SUPT1-CCR5 cells infected with HIV-$1_{NL4.3\text{-}BaL}$ in either the presence or absence of nevirapine (NVP). Supernatant was harvested at 4, 24, 48, or 72 hours to assay for IL-1β secretion. (**C**) MDMs from 5 independent donors were knocked out (KO) for *AAVS1 CARD8,* or *NLRP3* using a Synthego gene KO kit then immunoblotted using an anti-CARD8 antibody or anti-vinculin. Full-length and FIIND-processed CARD8 intermediates are marked with a purple arrow. Table between CARD8 and vinculin blot shows Synthego gene KO% scores for each donor KO line. (**D**) *AAVS1*, *CARD8* or *NLRP3* KO MDM lines from (C) were primed with Pam3CSK4 (500ng/mL) overnight and then cocultured with SUPT1-CCR5 cells mock-, or HIV-$1_{NL4.3\text{-}BaL}$-infected then assayed for inflammasome activation 48 hours post-coculture for IL-1β secretion. For all SUPT1:MDM experiments, SUPT1-CCR5 cells were infected with HIV-1_{LAI} or HIV-$1_{NL4.3\text{-}BaL}$ such that 5-20% of cells were positive for intracellular $p24^{gag}$ after 20 hours. IL-1 levels shown were normalized to the SUPT1 mock-infected coculture control. Dotted line indicates limit of detection (LoD). Datasets represent mean ± SD (A: n=3 independent donors, B: n=2 biological replicates for each donor, D: n=3 technical replicates per donor). One-way ANOVA with (A)Tukey's or (D) Sidak's test or (B) two-way ANOVA with Tukey's test using GraphPad Prism 10. ns = not significant, *p<0.05,**p<0.01, ***p<0.001, ****p<0.0001.

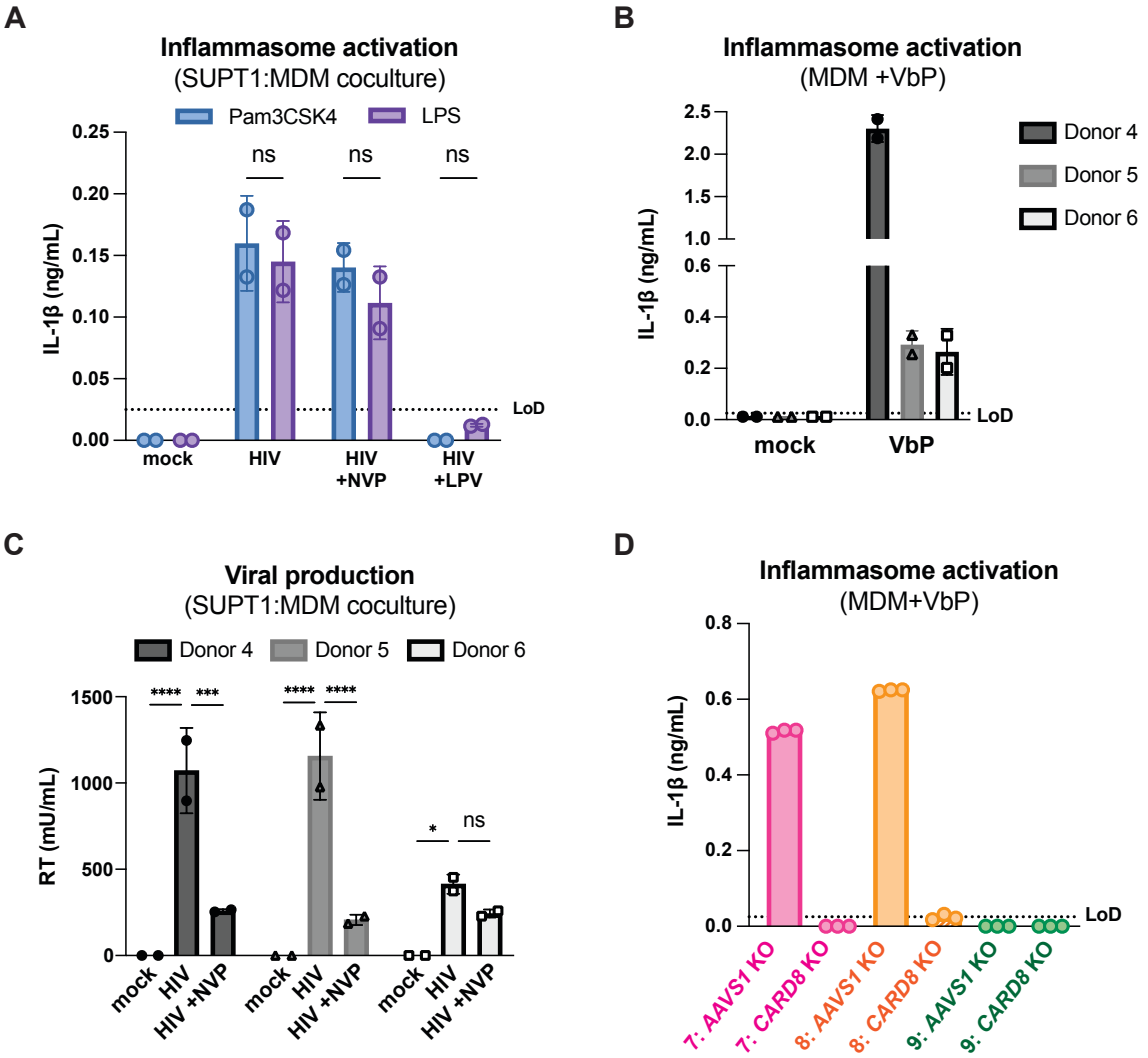

Figure 3– figure supplement 1: Cell-to-cell HIV infection induces CARD8-dependent activation in monocyte-derived macrophages (MDMs). (**A**) MDMs from donor 6 were primed with either 500ng/mL Pam3CSK4 or 5μg/mL LPS then cocultured with SUPT1-CCR5 cells that had been infected with HIV-$1_{NL4.3-BaL}$ 24 hours prior to coculture. Each coculture was started in the presence of DMSO, nevirapine (NVP) or lopinavir (LPV). Supernatant was harvested 72 hours post coculture to assay for IL-1β secretion. (**B**) MDMs from the same 3 independent blood donors assayed in Figure 3B were primed overnight with Pam3CSK4 then treated with 10μM VbP for 24 hours before assaying for IL-1β secretion via IL-1 reporter assay. (**C**) Supernatant from SUPT1:MDM coculture experiment done in Figure 3B was harvested at 48 hours post coculture to assay for infectious virions via reverse transcriptase (RT) assay. (**D**) *AAVS1* or *CARD8* KO MDMs from donor 7-9 assayed in Figure 3C were primed and treated with VbP for 24 hours then assayed for IL-1β secretion. IL-1 levels from VbP treatment were normalized to untreated mock control. Dotted line indicates limit of detection (LoD). Datasets represent mean ± SD (A: n=2 biological replicates for one donor, B-C: n=2 technical replicates for each independent donor, D: n=3 technical replicates per donor). Two-way ANOVA with (A) Sidak's or (C) Dunnett's test (using GraphPad Prism 10. ns = not significant, *p<0.05,**p<0.01, ***p<0.001, ****p<0.0001.

226
227

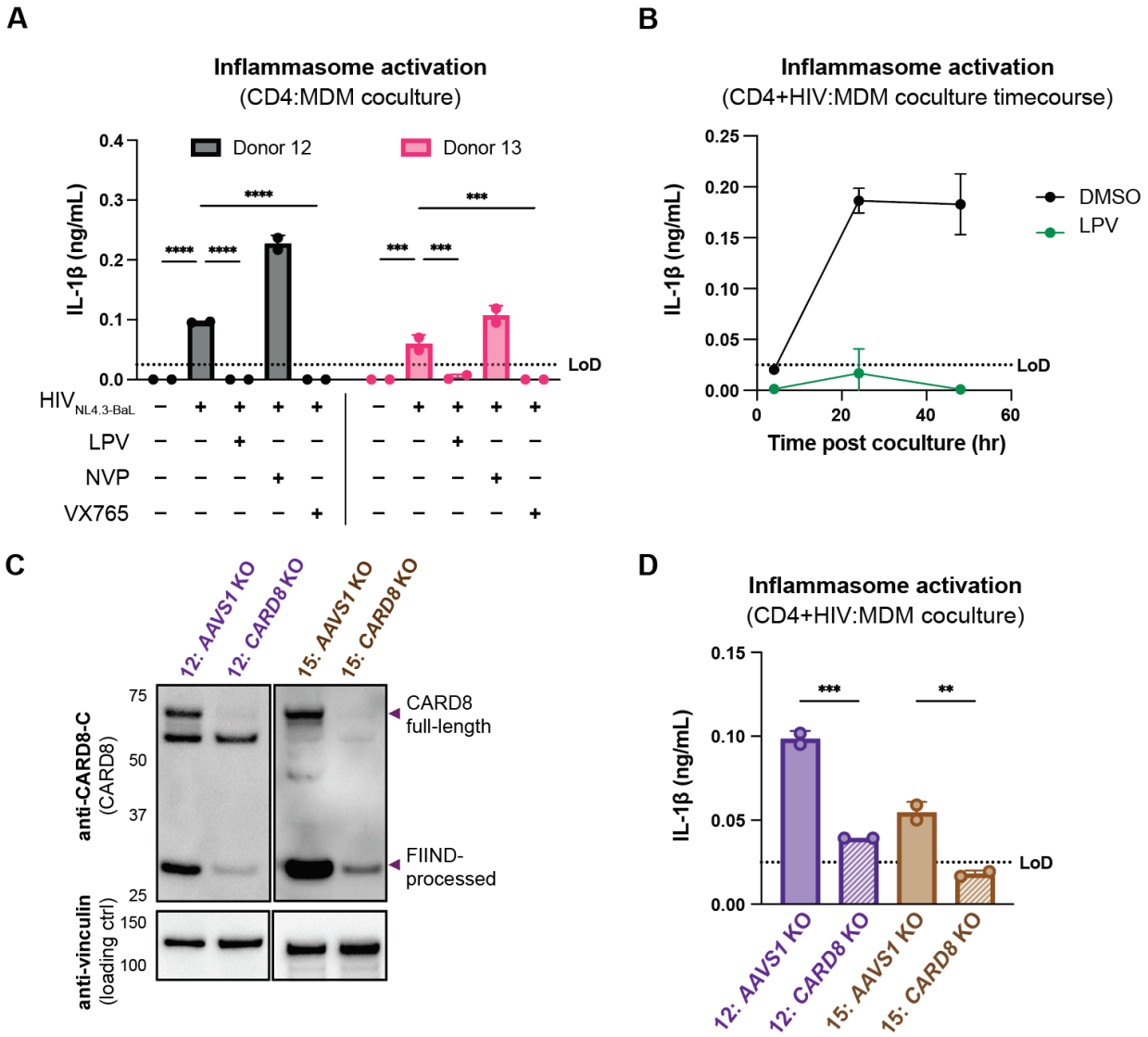

Figure 4. Primary CD4+ T cell:MDM coculture elicits CARD8-dependent inflammasome activation. (A) CD4+ T cells from a blood donor were isolated, activated, and either mock infected or infected with HIV-1$_{NL4.3-BaL}$ for 3 days such that ~10% of cells were positive for intracellular p24^{gag}. MDMs were primed with Pam3CSK4 then cocultured with mock or HIV-1 infected primary CD4 T cells in the presence or absence of lopinavir (LPV), nevirapine (NVP), or VX765, inhibiting HIV protease, reverse transcriptase, or caspase 1, respectively. Supernatants were harvest 3 days post coculture to assay for IL-1β secretion via IL-1 reporter assay. (**B**) CD4+ T cells from donor 12 and MDMs from donor 14 were cocultured as in A in the presence or absence of LPV. Supernatant was harvested at 4, 24 and 48 hours post coculture to probe for IL-1β secretion. (**C**) *AAVS1* or *CARD8* MDM KOs were immunoblotted using an anti-CARD8 antibody or anti-vinculin. Full-length and FIIND-processed CARD8 intermediates are marked with a purple arrow. (**D**) *AAVS1* or *CARD8* KO MDMs from (C) were cocultured with CD4+ T cells infected with HIV-1$_{NL4.3-BaL}$ then assayed for IL-1β secretion 48 hours post coculture. The donor 12 cocultures consisted of autologous CD4s and MDMs whereas the MDMs from donors 13-15 were cocultured with donor 12 CD4s. Dotted line indicates limit of detection (LoD). Datasets represent mean ± SD (A,D: n=2 technical replicates for each donor, B: n=3 technical replicates for one donor). (A) Two-way ANOVA with Tukey's test (D) One-way ANOVA with Sidak's test using GraphPad Prism 10. ns = not significant, *p<0.05,**p<0.01, ***p<0.001, ****p<0.0001.

229 **Coculture of HIV-1 infected primary CD4+ T cells with primary MDMs elicits CARD8-**
230 **dependent inflammasome activation**

231 We next investigated inflammasome activation in the context of cell-to-cell infection
232 using primary CD4+ T cells as donor cells, rather than SUPT1 cells, and primary MDMs as
233 target cells. Mock or HIV-$1_{NL4.3-BaL}$ infected CD4+ T cells were cocultured with MDMs in the
234 presence or absence of various inhibitors (as in **Figure 3A**). We assessed inflammasome
235 activation via IL-1β secretion 72 hours post coculture and observed inflammasome activation
236 when coculturing with HIV-infected T cells but not mock infected T cells or cocultures treated
237 with LPV or VX765, demonstrating that inflammasome activation is driven by HIV^{PR} and CASP1
238 (**Figure 4A**) and consistent with our findings using the SUPT1:MDM coculture (**Figure 3**). We
239 also observed that inflammasome activation persisted in NVP-treated cocultures, suggesting
240 that incoming protease is also important for inflammasome activation in the context of cell-to-cell
241 transmission of HIV-1 from primary CD4+ T cells to primary MDMs (**Figure 4A**). To confirm the
242 potency of LPV and NVP, we assayed for infectious virions in the supernatant of these
243 CD4:MDM cocultures and detected a dramatic decrease in RT activity in the presence of either
244 of these drugs, indicating that these drugs were efficacious at this dose (**Figure 4– figure**
245 **supplement 1A**). We also conducted a time course experiment with a CD4:MDM coculture from
246 an independent donor in the presence or absence of LPV. Similar to the SUPT1:MDM time
247 course (**Figure 3B**), we were able to detect elevated levels of IL-1β by 24 hours post coculture,
248 which was again strictly dependent on the enzymatic activity of the viral protease as LPV
249 treatment completely inhibited IL-1β secretion (**Figure 4B**).

250 To interrogate the specific role of CARD8 in this primary CD4:MDM coculture system,
251 we generated *AAVS1* (as a control) or *CARD8* KO MDMs and cocultured the MDMs with either
252 mock or HIV-infected primary CD4+ T cells then assayed for inflammasome activation 48 hours
253 post coculture. KO efficiency was confirmed via immunoblot and functional response to VbP (in
254 one of the two donors) (**Figure 4C, Figure 4–figure supplement 1B**). We detected a significant

255 decrease in inflammasome activation when infected T cells were cocultured with *CARD8* KO
256 versus *AAVS1* KO MDMs (**Figure 4D**), indicating that CARD8 is required for inflammasome
257 activation in MDMs during HIV-1 transmission from primary CD4+ T cells to MDMs. Taken
258 together, our data indicate that CARD8 plays a pivotal role in sensing and responding to HIV-1
259 cell-to-cell infection between primary CD4 T cells and macrophages.
260
261 ***Protease inhibitor resistant strains of HIV-1 differentially cleave and activate CARD8***
262 The consequences of CARD8 inflammasome activation on viral replication have been
263 challenging to assess given that viral fitness is intrinsically linked to viral protease processing of
264 the viral polyprotein such that inhibiting HIV^{PR} also prevents viral replication. In an attempt to

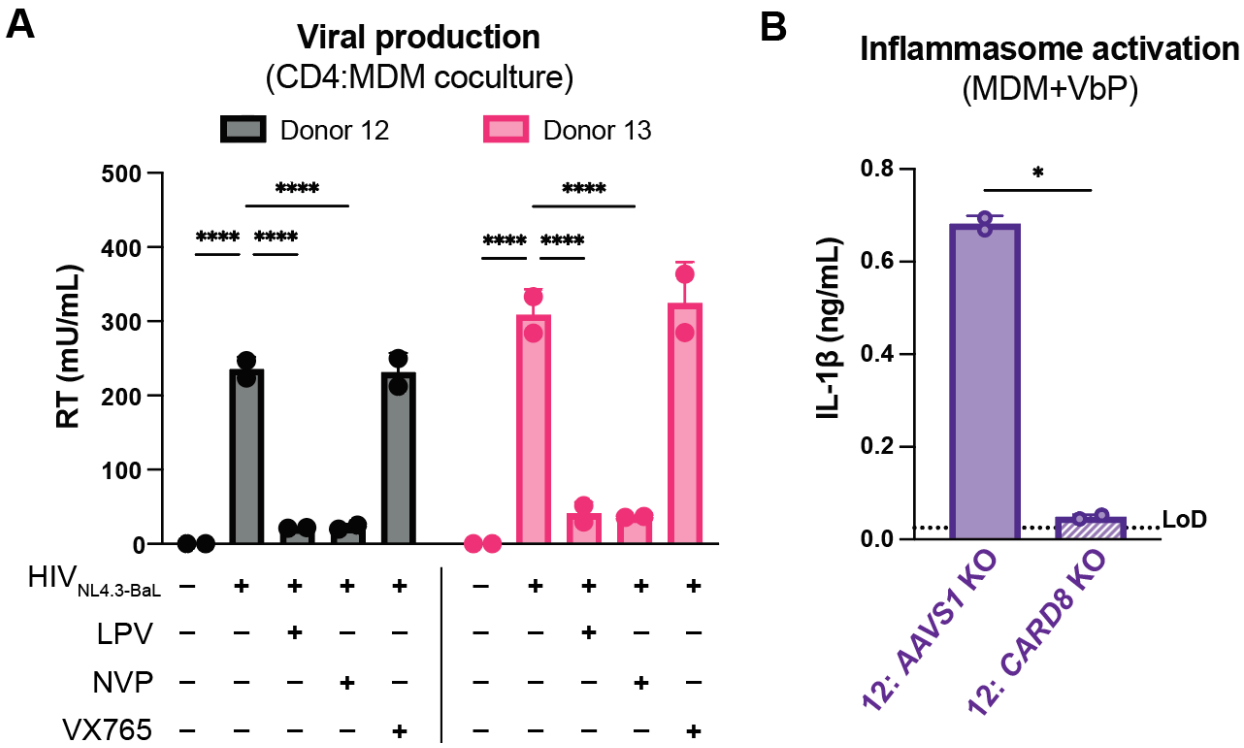

Figure 4– figure supplement 1. Primary CD4 T cell:MDM coculture elicits CARD8-dependent inflammasome activation. (**A**) Supernatant was harvested 72 hours post coculture from coculture described in Figure 4A then assayed for infectious virions via (RT) transcriptase assay. (**B**) *AAVS1* or *CARD8* KO MDMs from donor 12 were primed with Pam3CSK4 then treated with VbP for 24 hours and probed for IL-1β secretion. (n=2 technical replicates for each donor). (A) Two-way ANOVA with Tukey's test (B) One-way ANOVA with Sidak's test using GraphPad Prism 10. ns = not significant, *p<0.05,**p<0.01, ***p<0.001, ****p<0.0001.

265 circumvent this issue, we surveyed a panel of multi-HIV^{PR} inhibitor-resistant (PI-R) infectious
266 molecular clones of HIV-1 (Varghese et al., 2013). This panel of PI-R molecular clones vary in
267 resistance to HIV protease inhibitors including nelfinavir (NFV), fosamprenavir (FPV), saquinavir
268 (SQV), indinavir (IDV), atazanavir (ATV), lopinavir (LPV), tipranavir (TPV), and darunavir (DRV).
269 Each molecular clone encodes 4 to 11 mutations in HIV^{PR} as well as various compensatory
270 HIV^{gag} mutations (Varghese et al., 2013) (**Table S1**).

271 We initially tested if PI-R HIV-1 proviruses differentially cleave CARD8 by co-transfecting
272 HEK293T cells with an expression plasmid encoding an N-terminal mCherry tagged human
273 CARD8 and either wildtype HIV-1$_{LAI}$ or PI-R HIV-1 proviruses. HIV-1$_{LAI}$ protease cleaves CARD8
274 between phenylalanine (F) 59 and F60 (Wang et al 2021), resulting in a ~33kDa product
275 (**Figure 5A,** top). By quantifying the 33kDa CARD8 cleavage product with each HIV-1 provirus,
276 we identified a PI-R clone that exhibited similar efficiency at cleaving CARD8 to HIV-1$_{LAI}$ (i.e., PI-
277 R1), PI-R clones that were markedly less efficient at cleaving CARD8 than HIV-1$_{LAI}$ (i.e., PI-R2,
278 PI-R3, PI-R5, PI-R9, and PI-R10) and two PI-R clones, PI-R12 and PI-R13, that were more
279 efficient at cleaving CARD8 than HIV-1$_{LAI}$ (**Figure 5A,** top**, Table S1**). Of note, all PI-R
280 proviruses had similar levels of HIV^{PR} activity for HIV^{gagpol} polyprotein processing from p55^{gag} to
281 p24^{gag} as indicated by the ratio of p24^{gag}/p55^{gag} quantified from the anti-p24^{gag} immunoblot
282 (**Figure 5A,** middle). These results indicate that naturally occurring HIV-1 protease mutations
283 can influence host targets like CARD8.

284 We next assessed if PI-R clones exhibiting reduced (PI-R2 and -9) or increased (PI-R12
285 and -13) cleavage of CARD8 relative to HIV-1$_{LAI}$ (**Figure 5A and B**, and **Table S1**) resulted in
286 differential inflammasome activation. HEK293T cells endogenously express CARD8 but lack the
287 downstream components (i.e., CASP1, GSDMD, and IL-1β/IL18) of the inflammasome pathway.
288 Thus, we reconstituted the inflammasome pathway in HEK293T cells by co-transfection of
289 human caspase 1, human pro-IL-1β, and either empty vector, HIV-1$_{LAI}$ or representative PI-R
290 proviruses then quantified CASP1-dependent processing of pro-IL-1β as a readout of CARD8

291 inflammasome activation as in (Tsu et al., 2023). Consistent with the observed differences in
292 CARD8 cleavage by PI-R clones (**Figure 5A**), we found that PI-R2 and PI-R9, which exhibited
293 less CARD8 cleavage than HIV-1_{LAI}, also induced lower IL-1β levels than HIV-1_{LAI} (**Figure 5B**).
294 Similarly, PI-R12 and PI-R13, which demonstrated enhanced CARD8 cleavage, elicited higher
295 IL-1β levels than HIV-1_{LAI} (**Figure 5B**). However, these PI-R clones, relative to the LAI strain,
296 may have distinct protease substrate specificity, variable efficiency/kinetics in viral assembly,
297 gag dimerization, and other factors which may also influence CARD8 inflammasome activation.
298 We next assessed inflammasome activation by the PI-R clones in a cell-to-cell transmission
299 model using HEK293T cells as donor cells rather than SUPT1 cells and either WT or *CARD8*
300 KO THP-1 cells as the target line at a 1:1 ratio. We opted to overexpress the HIV-1_{LAI} or the PI-
301 R proviruses in HEK293T cells rather than infecting SUPT1 cells due to dramatic variability in
302 replication kinetics between PI-R strains. In these HEK293T:THP-1 cocultures, we observed
303 that cell-to-cell transmission of PI-R2 and PI-R9 resulted in lower IL-1β levels while PI-R12 and
304 PI-R13 resulted in higher IL-1β levels compared to HIV-1_{LAI}, respectively (**Figure 5C**),
305 consistent with our findings from CARD8 cleavage (**Figure 5A**) and reconstituted inflammasome
306 assays (**Figure 5B**). Our findings suggest that HIV-dependent inflammasome activation is under
307 genetic control of the viral protease in a manner that can be increased or decreased with
308 naturally occurring mutations induced by drug resistance.

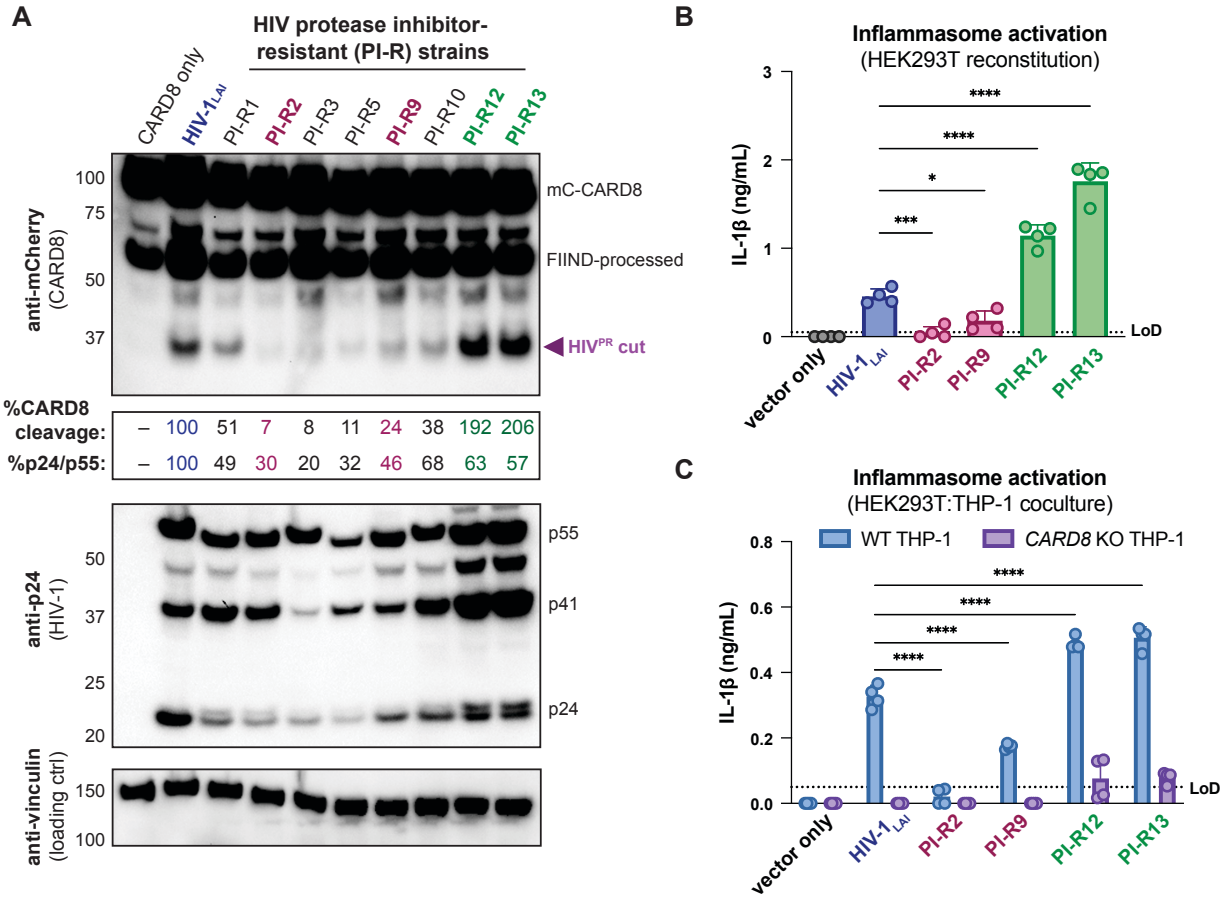

Figure 5. Protease inhibitor resistant strains of HIV-1 differentially cleave and activate CARD8. (**A**) HEK293T cells were transfected with a construct encoding CARD8 with an N-terminal mCherry tag (mCherry-CARD8) and indicated HIV-1 proviral constructs. Protease inhibitor-resistant (PI-R) clones of HIV-1 are a subset of a panel expressing prototypical multidrug resistant HIV-1 protease (HIV^{PR}) in an NL4.3 backbone (Table S1). Top: Immunoblotting using anti-mCherry antibody to detect mCherry-CARD8. The full-length (mC-CARD8) and FIIND-processed bands are indicated as well as the HIV^{PR} cut product. The band at ~45 kDa is the result of cleavage by the 20S proteasome (Hsiao et al., 2022). % CARD8 cleavage was calculated by quantifying the HIV^{PR} cut band relative to the HIV-1_{LAI} control using BioRad Image Lab 6. Middle: Immunoblotting with an anti-$p24^{gag}$ antibody showing HIV-1^{gag} cleavage products $p41^{gag}$ and $p24^{gag}$, and/or full-length HIV-1^{gag}, $p55^{gag}$. %p24/p55 was calculated from the ratio of $p24^{gag}$ versus $p55^{gag}$ product by quantifying the volume of the $p24^{gag}$ bands versus the $p55^{gag}$ band relative to the HIV-1_{LAI} control using BioRad Image lab 6. Bottom: Immunoblotting with an anti-vinculin antibody to detect vinculin as a loading control. (**B**) HEK293T cells were transfected with human caspase 1 and human pro-IL-1β, and either carrier vector or indicated HIV-1 proviruses then probed for IL-1β secretion 24 hours post-transfection via IL-1R reporter assay. (**C**) HEK293T cells were transfected with indicated HIV-1 proviruses (300ng). 24 hours post-transfection either wildtype (WT) or *CARD8* knockout (KO) THP-1s were overlayed on the transfected HEK293T cells in a 1:1 ratio. THP-1s were primed with Pam3CSK4 overnight prior to coculture. Supernatants were harvested 24 hours post coculture to assay for IL-1β secretion as in (B). Dotted line indicates limit of detection (LoD). Datasets represent mean ± SD (n=4 biological replicates). p-Values were determined by two-way ANOVA with Dunnett's test using GraphPad Prism 10. ns = not significant, *$p<0.05$,**$p<0.01$, ***$p<0.001$, ****$p<0.0001$.

310 **Table S1: Protease inhibitor resistance mutations and relative CARD8 cleavage.**

Clone name	Reported PI-resistance mutations in HIV^{PR}	HIV^{gag} mutation	Strongest PI-R[1]	% CARD8 cleavage (relative to HIV_{LAI})	Additional amino acid changes in HIV^{PR} relative to NL4.3
$HIV\text{-}1_{LAI}$	wildtype	wildtype	wildtype	100	37S
CA126802 (PI-R1)	11I, 32I, 33F, 46I, 47V, 54M, 58E, 73S, 84V, 89V, 90M	431V (NC/p1) 437N (NC/p1) 453LF (p1/p6)	FPV, LPV, TPV, DRV	51	10I, 12K, 13V, 20V, 35G, 36I, 37D, 57K, 63P, 64V, 66V, 7IV
CA122805 (PI-R2)	**10F, 33F, 43T, 46L, 54V, 82A, 84V, 90M**	**431V (NC/p1) 532S (p1/p6)**	**SQV**	**7**	16A,19I, 20R, 35D, 36L, 37D, 55R, 57K, 60E, 62V, 63P, 71V, 93L
CA126805 (PI-R3)	33F, 43T, 46I, 48V, 50V, 54S, 82A	437N (NC/p1) 449VF (p1/p6) PTAP insertion (p6)	SQV, IDV, LPV	**8**	not determined*
CA96457 (PI-R5)	48V, 53L, 54V, 82A, 90M	436R (NC/p1)	SQV	11	10I, 37D, 63P, 71T, 77I, 93L
CA96458 (PI-R9)	**10F, 30N, 33F, 43T, 84V, 88D, 90M**	**431V (NC/p1)**	**NFV, SQV**	**24**	15V, 35D, 36L, 37E, 60E, 62V, 63P
CA50834-1 (PI-R10)	24I, 46L, 54V, 76V, 82A	431V (NC/p1)	IDV, LPV	38	10I, 14R, 35D, 36I, 37E, 63P,71V
CA96451 (PI-R12)	**32I, 33F, 43T, 46I, 47V, 54M, 73S, 82A, 89V, 90M**	**437N (NC/p1) PTAP insertion (p6)**	**FPV, LPV**	**192**	10V, 12V, 13V, 15V, 20M, 60E, 61N, 62V, 63P, 67Y, 69K, 71I, 72L, 77I
CA20392-1 (PI-R13)	**24I, 46L, 54V, 82A**	**431V (NC/p1)**	**LPV**	**206**	10I, 14R, 35D, 36I, 37E, 63P, 71V

311 **Table S1** shows the protease inhibitor-resistant (PI-R) clones assayed in **Figure 5** with corresponding
312 mutations in HIV protease (HIV^{PR}) and HIV^{gag}. [1]These clones were previously cloned and assayed for PI-
313 R in (Varghese et al., 2013). The PI-R subset used in Figure 5B are bolded and highlighted in red or
314 green and denote either hypo- or hyper-active CARD8 cleavage, respectively. The last column reports
315 additional amino acid changes in the PI-R clones that were observed via whole plasmid Oxford Nanopore
316 sequencing. *We were unable to sequence verify PI-R3 due to poor plasmid quality. NFV-nelfinavir; FPV-
317 fosamprenavir; SQV- saquinavir; IDV- indinavir; LPV- lopinavir; TPV- tipranavir; DRV- darunavir. The
318 consensus subtype B sequence can be found on the Stanford HIV Drug Resistance Database (HIVDB)
319 ("Stanford - HIV Drug Resistance Database," n.d.). Relative CARD8 cleavage was determined by
320 quantifying band volume of the CARD8 cleavage product in BioRad Image Lab 6 and comparing to
321 cleavage with $HIV\text{-}1_{LAI}$.
322

323 **DISCUSSION**

324 We demonstrate that cell-to-cell transmission of HIV-1 from T cells to myeloid cells in both
325 immortalized and primary cell coculture models of infection yields CARD8-dependent
326 inflammasome activation via incoming HIV^{PR}. This inflammasome activation occurs in a largely
327 NLRP3-independent manner. In addition, we identified protease inhibitor resistant strains of
328 HIV-1 that differentially cleave and activate the CARD8 inflammasome. Thus, HIV^{PR} mutants
329 selected for their resistance to different protease inhibitors also affect their ability to cleave host
330 proteins including the inflammasome-forming sensor CARD8.

331

332 ***CARD8 is the primary inflammasome-forming sensor of HIV-1 infection***

333 Previously, both the NLRP3 and IFI16 inflammasomes have been implicated as innate
334 sensors of HIV-1 infection and drivers of CD4+ T cell depletion using blood and lymphoid-
335 derived CD4+ T cells, respectively, and cell-to-cell transmission was reported to be crucial for
336 IFI16 sensing of abortive HIV transcripts (Doitsh et al., 2014; Galloway et al., 2015; Monroe et
337 al., 2014; Zhang et al., 2021). However, the mechanism of NLRP3 inflammasome activation in
338 response to HIV-1 remains elusive. Similarly, there have been reports that IFI16 is not an
339 inflammasome-forming sensor, and instead a nuclear transcriptional regulator of antiviral genes
340 including type I interferons and RIG-I (Hornung et al., 2009; Jiang et al., 2021; Thompson et al.,
341 2014), suggesting that there may be other mechanisms of CD4+ T cell depletion and HIV-
342 dependent inflammasome activation at play. Indeed, CARD8, which is expressed and functional
343 in naïve and memory CD4+ and CD8+ T cells (Linder et al., 2020), was recently shown to be
344 required for pyroptosis in primary human blood- and lymphoid-derived CD4+ T cells and
345 humanized mouse models (Wang et al., 2024), implicating CARD8 as a major driver of CD4+ T
346 cell depletion during HIV-1 infection. In this study and our prior work (Kulsuptrakul et al., 2023),
347 we demonstrate that CARD8 is also the primary innate sensor during HIV-1 infection in myeloid
348 cell types during cell-to-cell transmission. However, our present study does not rule out the

349 possibility that under certain conditions or in certain cell types, NLRP3 inflammasome activation
350 may occur, for example following GSDMD pore formation following CARD8 inflammasome
351 activation and play a more profound role in promoting HIV-dependent inflammation.
352 Nonetheless, these data along with other recent work (Wang et al., 2024) strongly suggest that
353 CARD8 is a major innate sensor of HIV-1 infection.
354
355 ***Protease inhibitor resistance mutations and inflammatory disease***
356 Given the important role of HIV^{PR} in replication, early combination antiretroviral therapy for
357 people living with HIV (PLWH) included protease inhibitors along with RT inhibitors. However,
358 resistance mutations to protease inhibitors quickly arose in PLWH through mutations around the
359 HIV^{PR} active site allowing for polyprotein processing and viral maturation while avoiding drug
360 inhibition. Despite typically having poor overall viral fitness due to less efficient polyprotein
361 processing and replication relative to wildtype HIV-1 in the absence of protease inhibitors, these
362 mutant drug-resistant HIV-1 strains can persist in PLWH on antiviral therapy, posing a major
363 threat to controlling disease progression (De Luca, 2006; Martinez-Picado et al., 1999; Prado et
364 al., 2002; Resch et al., 2002). To compensate for mutations in HIV^{PR} that change its substrate
365 specificity, HIV^{gag} sometimes evolves mutations around HIV^{PR} cleavage sites to permit proper
366 polyprotein processing (Varghese et al., 2013). Here, we identified multiple HIV^{PR} inhibitor-
367 resistant strains of HIV-1 that can differentially cleave and activate the CARD8 inflammasome
368 (**Figure 5, Table S1**). As the degree of inflammation is a better predictor of disease progression
369 in untreated individuals than viral load (Deeks et al., 2004; Giorgi et al., 1999), we speculate that
370 differential CARD8 inflammasome activation could influence disease progression for PLWH
371 harboring HIV^{PR} resistance mutations that cleave CARD8 more or less efficiently. More broadly,
372 we suggest that host targets of viral proteases like CARD8 may influence the selection of viral
373 variants during treatment with antiviral protease inhibitor monotherapies.
374

375 ***Viral protease influx activates the CARD8 inflammasome***

376 In this study, we found that HIV-dependent CARD8 inflammasome activation during cell-
377 free infection requires a cationic polymer like DEAE-dextran to facilitate efficient viral infection
378 (see **Supplemental Note**). Despite being infected with the same amount of virus and exhibiting
379 similar percent infection 24 hours post-infection, as measured by intracellular $p24^{gag}$, with and
380 without DEAE-dextran, we hypothesize that DEAE-dextran during cell-free infection may
381 increase the total viral dose that enters cells consisting of both infectious particles and non-
382 infectious particles that may nonetheless contain active protease, leading to more efficient viral
383 protease influx to trigger CARD8 sensing. Hence, the percentage of $p24^{gag}$ positive cells after 24
384 hours may be an underestimate of total amount of viral entry in the DEAE-dextran condition. We
385 speculate that a considerable influx of incoming HIV^{PR} may be necessary to induce CARD8
386 inflammasome activation.

387 We also observed that DEAE-dextran can trigger inflammasome activation in some THP-1
388 cell lines (see **Supplemental Note**), prompting us to assay for inflammasome activation upon
389 HIV-1 cell-to-cell transmission with target cells at a 1:1 ratio in the absence of cationic polymer.
390 We found that inflammasome activation following cell-to-cell transmission of HIV-1 could be
391 detected by 24 hours (**Figure 3B**), which is delayed relative to our detection of CARD8
392 inflammasome activation 2 hours post cell-free HIV-1 infection in the presence of DEAE-dextran
393 (Kulsuptrakul et al., 2023). Nonetheless, we still hypothesize that this inflammasome activation
394 is driven by active incoming viral protease because treatment with an RT inhibitor has no effect
395 on inflammasome activation, which implies that *de novo* protease production is not necessary
396 (**Figure 3A and B, Figure 4A and B**). Similarly, we observed that IL-1β levels do not increase
397 after plateauing 24 hours after establishing the coculture (**Figure 3B, Figure 4B**), suggesting
398 that secondary infection does not further amplify inflammasome activation. We infer that this is
399 also likely a product of the efficiency of viral entry and the necessity for multiple virions infecting
400 at the same time to deliver a sufficient amount of active HIV^{PR} for cytosolic CARD8 sensing. We

401 postulate that under certain physiological conditions, cell-to-cell transmission can cause CARD8
402 inflammasome activation when there is an influx of active incoming HIV^{PR} across the viral
403 synapse. Taken together, we speculate that both cell-free infection facilitated by cationic
404 polymer or cell-to-cell transmission can achieve sufficient levels of active HIV^{PR} influx to activate
405 the CARD8 inflammasome.

406 Macrophages have been reported to be primarily infected through phagocytosis of
407 infected CD4+ T cells or cell-to-cell transmission (Dupont and Sattentau, 2020; Martínez-
408 Méndez et al., 2017; Orenstein, 2000). We demonstrate that unlike CD4+ T cells, which are
409 rapidly depleted by HIV-1 infection and do not release IL-1β or IL-18 (Linder et al., 2020),
410 primary macrophages release pro-inflammatory cytokines in response to HIV^{PR} during cell-to-
411 cell infection from primary CD4+ T cells and T cell lines (**Figure 3, Figure 4**), thus representing
412 a potential source of sustained IL-1β and subsequent chronic immune activation. In addition to
413 promoting chronic immune activation, HIV-dependent IL-1β release from macrophages may
414 also contribute to HIV-1 pathogenesis by activating nearby CD4+ T cells, rendering them
415 susceptible to becoming infected with HIV-1, and thus indirectly promoting CD4+ T cell
416 depletion. Collectively with our prior work (Kulsuptrakul et al., 2023), our findings provide further
417 evidence that CARD8 inflammasome activation is driven by incoming HIV^{PR} under conditions
418 where multiple virions may enter cells, and thus could be a potential driver of HIV-1
419 pathogenesis by promoting chronic immune activation.

420

421 **METHODS**

422 ***Plasmids and Reagents***

423 pMD2.G used for HIV-$1_{LAI\text{-}VSVG}$ production was a gift from Didier Trono (Addgene). HIV-1_{LAI} has
424 been previously described (Peden et al., 1991). The following reagents were obtained through
425 the NIH HIV Reagent Program, Division of AIDS, NIAID, NIH: lopinavir (LPV), nevirapine (NVP),

426 Human Immunodeficiency Virus 1 (HIV-1) NL4-3 BaL Infectious Molecular Clone (p20-36) (HIV-
427 $1_{NL4.3\text{-}BaL}$), ARP-11442, contributed by Dr. Bruce Chesebro (Chesebro et al., 1992, 1991; Toohey
428 et al., 1995; Walter et al., 2005), and Panel of Multi-Protease Inhibitor Resistant Infectious
429 Molecular Clones, HRP-12740, contributed by Dr. Robert Shafer (Varghese et al., 2013). Mutant
430 HIV^{PR} sequences were amplified from clinically-derived viral cDNA encoding protease genes
431 with resistance to multiple PRis then cloned into an NL4.3 backbone with overhangs including
432 the 3' end of gag with the gag cleavage site and the 5' end of RT as previously described
433 (Varghese et al., 2013). CARD8 variant constructs were cloned as previously described
434 (Kulsuptrakul et al., 2023). VX765 and MCC950 were sourced from Invivogen (cat: inh-vx765i-1
435 and inh-mcc, respectively).
436
437 ***Cell culture***
438 SUPT1 (ATCC) and THP-1 cells (JK and ATCC) were cultured in RPMI (Invitrogen) with 10%
439 FBS, 1% penicillin/streptomycin antibiotics, 10 mM HEPES, 0.11 g/L sodium pyruvate, 4.5 g/L
440 D-glucose and 1% Glutamax. JK THP-1 cells were used for all experiments in this manuscript
441 and our previous work unless explicitly stated (see **Supplemental Note**) (Kulsuptrakul et al.,
442 2023). Primary monocytes were cultured in RPMI (Invitrogen) with 10% FBS, and 1%
443 penicillin/streptomycin antibiotics and differentiated in the presence of 20ng/mL GM-CSF
444 (Peprotech cat: 300-03) and 20ng/mL M-CSF (Peprotech cat: 300-25). Primary CD4+ T cells
445 were cultured in RPMI (Invitrogen) with 10% FBS, 1% penicillin/streptomycin antibitiocs and
446 100U/mL IL-2. HEK293T (ATCC) lines were cultured in DMEM (Invitrogen) with 10% FBS and
447 1% penicillin/streptomycin antibiotics. All lines routinely tested negative for mycoplasma bacteria
448 (Fred Hutch Specimen Processing & Research Cell Bank). SUPT1 and THP-1 cell lines were
449 authenticated by STR profiling analysis (Fred Hutch Genomics core and TransnetYX, Inc.) (see
450 **Supplemental Note**).
451

452 ***HIV-1$_{LAI}$, HIV-1$_{LAI\text{-}VSVG}$, and HIV-1$_{NL4.3\text{-}BaL}$ production***

453 293T cells were seeded at 2-3×10^5 cells/well in six-well plates the day before transfection using
454 TransIT-LT1 reagent (Mirus Bio LLC) at 3 µL transfection reagent/well as previously described
455 (OhAinle et al., 2018). For HIV-1 production, 293Ts were transfected with 1 µg/well HIV$_{LAI}$ or
456 HIV-1$_{NL4.3\text{-}BaL}$ proviral DNA or 1 µg/well HIV$_{LAI}$ Δenv DNA and 500 ng/well pMD2.G for HIV-1$_{LAI}$,
457 HIV-1$_{NL4.3\text{-}BaL}$, and HIV-1$_{LAI\text{-}VSVG}$, respectively. One day post-transfection, media was replaced.
458 Two days post-transfection, viral supernatants were collected and filtered through a 20 µm filter
459 and aliquots were frozen at –80°C. HIV-1$_{LAI}$, HIV-1$_{NL4.3\text{-}BaL}$ and HIV-1$_{LAI\text{-}VSVG}$ proviruses were
460 previously described (Bartz and Vodicka, 1997; Gummuluru et al., 2003; Peden et al., 1991).
461

462 ***Cell-free and cell-to-cell coculture HIV-1 infection***

463 Cell-free infections with HIV-1$_{LAI\text{-}VSVG}$ were done as previously described (Kulsuptrakul et al.,
464 2023). Subsequent cell death was assessed by incubating in media containing propidium iodide
465 dye (10µg/mL) for 5 minutes at room temperature then washed once with PBS before fixing with
466 BD CytoFix/Cytoperm (cat:BDB554714) and staining for intracellular p24^{gag} (Beckman Coulter
467 cat#: 6604665) for flow cytometry. In the HIV-1 cell-to-cell transmission system, SUPT1
468 expressing CCR5 (SUPT1-CCR5) cells were spinoculated at 1100g for 30min with either HIV-
469 1$_{LAI}$ or HIV-1$_{NL4.3\text{-}BaL}$ in the presence of 10µg/mL DEAE-dextran. SUPT1-CCR5 cells were
470 lentiviral transduced to express CCR5 (Dingens et al., 2017). After 24 hours, mock or HIV-1
471 infected SUPT1-CCR5 cells were washed three times in PBS such that DEAE-dextran and cell-
472 free virus were removed before starting coculture with THP-1 cells or MDMs. THP-1 cells and
473 MDMs were seeded at 5 x 10^5 cells/well and primed with 500ng/mL Pam3CSK4 (Invivogen) for
474 16-24 hours before coculture. Mock or infected SUPT1 cells were seeded at 5 x 10^5 cells/well.
475 Cultured supernatants from coculture were harvested 48 hours after starting the coculture for
476 the IL-1R reporter assay, which was previously described (Kulsuptrakul et al., 2023).
477

478 ***Transwell coculture HIV-1 infection***

479 SUPT1 cells were spinoculated at 1100g for 30min with HIV-1_{LAI} in the presence of 10µg/mL
480 DEAE-dextran. After 24 hours, mock or HIV-1 infected SUPT1 cells were washed 3 times in
481 PBS and either mixed in a 24-well with THP-1 cells or placed in a transwell insert above target
482 THP-1 cells at a concentration of 5 x 10^5 infected SUPT1 cells and 2.5 x 10^5 THP-1 cells per
483 well. THP-1 cells were primed overnight with 500ng/mL Pam3CSK4 before starting coculture.
484 The transwell insert has a 0.4µm membrane at the bottom of the well (ThinCert™ Tissue
485 Culture Inserts, Sterile, Greiner Bio-One cat:665640), allowing virus to pass out of the transwell
486 but not the infected cell. Reverse transcriptase (RT) activity in viral supernatants was measured
487 using the RT activity assay as previously described (Roesch et al., 2018; Vermeire et al., 2012).
488 A stock of HIV-1_{LAI} virus was titered multiple times, aliquoted at −80°C and used as the standard
489 curve in all assays.
490

491 ***Monocyte-derived macrophage isolation, differentiation, and editing***

492 Primary monocytes were isolated via negative selection using the EasySep™ Human Monocyte
493 Isolation Kit (Easy Sep, 1x10^9) (Stem Cell Technologies) according to the manufacturer's
494 protocols from PBMCs collected from blood donors. Upon isolation, monocytes were seeded at
495 1 x 10^6 cell/mL and differentiated for 5 days in the presence of media containing 20ng/mL GM-
496 CSF (Peprotech cat: 300-03) and 20ng/mL M-CSF (Peprotech cat: 300-25), changing media
497 every other day. For edited MDMs, isolated monocytes were electroporated in cuvettes (100µL)
498 with 2.5-5 x 10^6 cells/nucleofection in the presence of pre-complexed Cas9-RNPs (300pmol
499 sgRNA: 100pmol Cas9) in Lonza P2 buffer using pulse code DK-100. RNPs were complexed
500 with sgRNA from the Synthego gene KO kit, which includes 3 sgRNAs per gene. Thus, each
501 sgRNA was present at a 1:1 ratio with Cas9 (QB3 MacroLab or Synthego SpCas9 2NLS
502 Nuclease). A table of sgRNAs used for *AAVS1*, *CARD8,* or *NLRP3* KO can be found in **Table**
503 **S2** below. After nucleofection, cells were supplemented with 900µL of prewarmed media and

504 allowed to recover for 30 minutes at 37°C before counting and seeding at ~1-1.5x10^6 cells/mL
505 for differentiation. Media was changed 24 hours post nucleofection then differentiated for 5 more
506 days before characterizing knockout efficiency and conducting coculture experiments.

507 **Table S2:**

sgRNA	Sequence
CARD8 sgRNA1	CUCUGCAGUGACAUCAAACA
CARD8 sgRNA2	UGACGAUUGCGUUUGGUUCC
CARD8 sgRNA3	AGCGUUUGGUUCCCCACUGC
AAVS1 sgRNA 1	GUUAAUGUGGCUCUGGUUCU
AAVS1 sgRNA 2	ACCCCACAGUGGGGCCACUA
AAVS1 sgRNA 3	CCUUCCUAGUCUCCUGAUAU
NLRP3 sgRNA 1	GCUCAGAAUGCUCAUCAUCG
NLRP3 sgRNA 2	GAUGAUGUUGGACUGGGCAU
NLRP3 sgRNA 3	CAAGGCUCACCUCCCGACAG

508

509 ***CD4+ T cell isolation, infection, and coculture***

510 Primary CD4+ T cells were isolated via positive selection using the EasySep™ Release Human
511 CD4 Positive selection kit (Stem Cell Technologies Cat: 17752) according to the manufacturer's
512 instructions from PBMCs collected from blood donors and seeded at 2.5x10^6 cells/mL in the
513 presence of 100U/mL IL-2. T cells were activated 24 hours post-isolation with CD3/CD28
514 activation beads (Miltenyi Biotech Cat: 130-091-441). Activation beads were removed according
515 to the manufacturer's protocols 24 hours later for infection. For infection, T cells were
516 suspended at 1-1.5x10^6 cells/mL in 15mL conical tubes containing 8μg/mL polybrene, 100U/mL
517 IL-2, and HIV-$1_{NL4.3\text{-}BaL}$ then spinoculated at 1100g at 30°C for 90 min. Three days post-infection,
518 CD4s were assessed for intracellular $p24^{gag}$ via flow cytometry (~10% infected) then washed
519 thrice with PBS before coculturing with MDMs. CD4:MDM coculture RPMI media was
520 supplemented with 100U/mL IL-2, 20ng/mL GM-CSF, 20ng/mL M-CSF, and 500ng/mL
521 Pam3CSK4.

522

523 ***CARD8 cleavage assay***

524 HEK293T cells were seeded at 1–1.5 × 10^5 cells/well in 24-well plates the day before
525 transfection using TransIT-LT1 reagent at 1.5 µL transfection reagent/well (Mirus Bio LLC). One
526 hundred ng of indicated constructs encoding an N-terminal mCherry-tagged CARD8 were co-
527 transfected into HEK293T cells with empty vector ('–'), HIV_{LAI} or PI-R provirus. To normalize
528 HIV^{gag} expression between HIV-1_{LAI} and the PI-R clones, which are in a different vector
529 backbone, 400ng of HIV-1_{LAI} and 200ng of all PI-R clones were transfected. All conditions were
530 normalized with empty vector to contain the same amount of DNA. Cytoplasmic lysates were
531 harvested 24 hours post-transfection and immunoblotted as previously described (Kulsuptrakul
532 et al., 2023).

533

534 ***HEK reconstitution assay***

535 HEK293T cells, which endogenously express CARD8, were seeded at 2.25 x 10^5 cell/well in 24-
536 well plates the day before transfection using TransIT-LT1 reagent at 1.5uL transfection
537 reagent/well (Mirus Bio LLC). Functional inflammasomes were reconstituted by transfecting in
538 5ng human CASP1 and 100ng human IL-1β. To assess the effects of different viral proteases
539 on inflammasome activation, HIV-1_{LAI} or PI-R clones were co-transfected in with CASP1 and IL-
540 1β. As with the CARD8 cleavage assay, a higher amount of 250ng HIV-1_{LAI} was added relative
541 to the PI-R clones, which were all added at 125ng, to normalize HIV^{gag} expression between the
542 different vector backbones. All conditions were normalized with empty vector to contain the
543 same amount of DNA. Cultured supernatant was harvested 24 hours post-transfection to assay
544 for IL-1β secretion via IL-1R reporter assay.

545

546 **Acknowledgements**

547 We thank everyone in the Emerman and Mitchell labs for helpful feedback on the project, Terry
548 Hafer and Marisa Yonemitsu for critical reading of the manuscript, Liang Shan and his lab

549 members for discussions and sharing of unpublished results and protocols, and the Fred
550 Hutchinson Shared Resources Genomics, Flow Cytometry, and Specimen Processing &
551 Research Cell Bank cores. LPV (HRP-9481), NVP (HRP-4666) and p24^{gag} antibody (ARP-3537)
552 were provided by the AIDS Reagent Program, Division of AIDS, NIAID, NIH. PSM is an HHMI
553 Freeman Hrabowski Scholar and is supported by grants from the National Institutes of Health
554 (NIH) (DP2 AI 154432-01) and the Mallinckrodt Foundation to PSM. ME is supported by NIH
555 grant DP1 DA051110. JK is supported by the University of Washington Cellular and Molecular
556 Biology Training Grant (T32 GM007270).

557 **References**

558 Abela IA, Berlinger L, Schanz M, Reynell L, Günthard HF, Rusert P, Trkola A. 2012. Cell-Cell
559 Transmission Enables HIV-1 to Evade Inhibition by Potent CD4bs Directed Antibodies.
560 *PLOS Pathog* **8**:e1002634. doi:10.1371/journal.ppat.1002634
561 Agosto LM, Herring MB, Mothes W, Henderson AJ. 2018. HIV-1-Infected CD4+ T Cells
562 Facilitate Latent Infection of Resting CD4+ T Cells through Cell-Cell Contact. *Cell Rep*
563 **24**:2088–2100. doi:10.1016/j.celrep.2018.07.079
564 Agosto LM, Uchil PD, Mothes W. 2015. HIV cell-to-cell transmission: effects on pathogenesis
565 and antiretroviral therapy. *Trends Microbiol* **23**:289–295. doi:10.1016/j.tim.2015.02.003
566 Bailey CA, Miller DK, Lenard J. 1984. Effects of DEAE-dextran on infection and hemolysis by
567 VSV. Evidence that nonspecific electrostatic interactions mediate effective binding of
568 VSV to cells. *Virology* **133**:111–118. doi:10.1016/0042-6822(84)90429-x
569 Bandera A, Masetti M, Fabbiani M, Biasin M, Muscatello A, Squillace N, Clerici M, Gori A,
570 Trabattoni D. 2018. The NLRP3 Inflammasome Is Upregulated in HIV-Infected
571 Antiretroviral Therapy-Treated Individuals with Defective Immune Recovery. *Front*
572 *Immunol* **9**.
573 Bartz SR, Vodicka MA. 1997. Production of High-Titer Human Immunodeficiency Virus Type 1
574 Pseudotyped with Vesicular Stomatitis Virus Glycoprotein. *Methods* **12**:337–342.
575 doi:10.1006/meth.1997.0487
576 Baxter AE, Russell RA, Duncan CJA, Moore MD, Willberg CB, Pablos JL, Finzi A, Kaufmann
577 DE, Ochsenbauer C, Kappes JC, Groot F, Sattentau QJ. 2014. Macrophage infection via
578 selective capture of HIV-1-infected CD4+ T cells. *Cell Host Microbe* **16**:711–721.
579 doi:10.1016/j.chom.2014.10.010
580 Brenchley JM, Paiardini M, Knox KS, Asher AI, Cervasi B, Asher TE, Scheinberg P, Price DA,
581 Hage CA, Kholi LM, Khoruts A, Frank I, Else J, Schacker T, Silvestri G, Douek DC.
582 2008. Differential Th17 CD4 T-cell depletion in pathogenic and nonpathogenic lentiviral
583 infections. *Blood* **112**:2826–2835. doi:10.1182/blood-2008-05-159301
584 Brenchley JM, Price DA, Schacker TW, Asher TE, Silvestri G, Rao S, Kazzaz Z, Bornstein E,
585 Lambotte O, Altmann D, Blazar BR, Rodriguez B, Teixeira-Johnson L, Landay A, Martin
586 JN, Hecht FM, Picker LJ, Lederman MM, Deeks SG, Douek DC. 2006. Microbial
587 translocation is a cause of systemic immune activation in chronic HIV infection. *Nat Med*
588 **12**:1365–1371. doi:10.1038/nm1511

589 Broz P, Dixit VM. 2016. Inflammasomes: mechanism of assembly, regulation and signalling. *Nat*
590 *Rev Immunol* **16**:407–420. doi:10.1038/nri.2016.58
591 Castro LK, Daugherty MD. 2023. Tripping the wire: sensing of viral protease activity by CARD8
592 and NLRP1 inflammasomes. *Curr Opin Immunol* **83**:102354.
593 doi:10.1016/j.coi.2023.102354
594 Chen P, Hübner W, Spinelli MA, Chen BK. 2007. Predominant mode of human
595 immunodeficiency virus transfer between T cells is mediated by sustained Env-
596 dependent neutralization-resistant virological synapses. *J Virol* **81**:12582–12595.
597 doi:10.1128/JVI.00381-07
598 Chesebro B, Nishio J, Perryman S, Cann A, O'Brien W, Chen IS, Wehrly K. 1991. Identification
599 of human immunodeficiency virus envelope gene sequences influencing viral entry into
600 CD4-positive HeLa cells, T-leukemia cells, and macrophages. *J Virol* **65**:5782–5789.
601 doi:10.1128/JVI.65.11.5782-5789.1991
602 Chesebro B, Wehrly K, Nishio J, Perryman S. 1992. Macrophage-tropic human
603 immunodeficiency virus isolates from different patients exhibit unusual V3 envelope
604 sequence homogeneity in comparison with T-cell-tropic isolates: definition of critical
605 amino acids involved in cell tropism. *J Virol* **66**:6547–6554. doi:10.1128/JVI.66.11.6547-
606 6554.1992
607 Chivero ET, Guo M-L, Periyasamy P, Liao K, Callen SE, Buch S. 2017. HIV-1 Tat Primes and
608 Activates Microglial NLRP3 Inflammasome-Mediated Neuroinflammation. *J Neurosci*
609 **37**:3599–3609. doi:10.1523/JNEUROSCI.3045-16.2017
610 Chun T-W, Carruth L, Finzi D, Shen X, DiGiuseppe JA, Taylor H, Hermankova M, Chadwick K,
611 Margolick J, Quinn TC, Kuo Y-H, Brookmeyer R, Zeiger MA, Barditch-Crovo P, Siliciano
612 RF. 1997a. Quantification of latent tissue reservoirs and total body viral load in HIV-1
613 infection. *Nature* **387**:183–188. doi:10.1038/387183a0
614 Chun T-W, Finzi D, Margolick J, Chadwick K, Schwartz D, Siliciano RF. 1995. In vivo fate of
615 HIV-1-infected T cells: Quantitative analysis of the transition to stable latency. *Nat Med*
616 **1**:1284–1290. doi:10.1038/nm1295-1284
617 Chun T-W, Stuyver L, Mizell SB, Ehler LA, Mican JAM, Baseler M, Lloyd AL, Nowak MA, Fauci
618 AS. 1997b. Presence of an inducible HIV-1 latent reservoir during highly active
619 antiretroviral therapy. *Proc Natl Acad Sci* **94**:13193–13197.
620 doi:10.1073/pnas.94.24.13193
621 Clark KM, Kim JG, Wang Q, Gao H, Presti RM, Shan L. 2022. Chemical inhibition of DPP9
622 sensitizes the CARD8 inflammasome in HIV-1-infected cells. *Nat Chem Biol* 1–9.
623 doi:10.1038/s41589-022-01182-5
624 Coll RC, Robertson AAB, Chae JJ, Higgins SC, Muñoz-Planillo R, Inserra MC, Vetter I, Dungan
625 LS, Monks BG, Stutz A, Croker DE, Butler MS, Haneklaus M, Sutton CE, Núñez G, Latz
626 E, Kastner DL, Mills KHG, Masters SL, Schroder K, Cooper MA, O'Neill LAJ. 2015. A
627 small-molecule inhibitor of the NLRP3 inflammasome for the treatment of inflammatory
628 diseases. *Nat Med* **21**:248–255. doi:10.1038/nm.3806
629 Collman R, Godfrey B, Cutilli J, Rhodes A, Hassan NF, Sweet R, Douglas SD, Friedman H,
630 Nathanson N, Gonzalez-Scarano F. 1990. Macrophage-tropic strains of human
631 immunodeficiency virus type 1 utilize the CD4 receptor. *J Virol* **64**:4468–4476.
632 doi:10.1128/jvi.64.9.4468-4476.1990
633 Collman R, Hassan NF, Walker R, Godfrey B, Cutilli J, Hastings JC, Friedman H, Douglas SD,
634 Nathanson N. 1989. Infection of monocyte-derived macrophages with human
635 immunodeficiency virus type 1 (HIV-1). Monocyte-tropic and lymphocyte-tropic strains of
636 HIV-1 show distinctive patterns of replication in a panel of cell types. *J Exp Med*
637 **170**:1149–1163. doi:10.1084/jem.170.4.1149

638 Conant D, Hsiau T, Rossi N, Oki J, Maures T, Waite K, Yang J, Joshi S, Kelso R, Holden K,
639 Enzmann BL, Stoner R. 2022. Inference of CRISPR Edits from Sanger Trace Data.
640 *CRISPR J* **5**:123–130. doi:10.1089/crispr.2021.0113
641 De Luca A. 2006. The impact of resistance on viral fitness and its clinical implications In: Geretti
642 AM, editor. Antiretroviral Resistance in Clinical Practice. London: Mediscript.
643 Deeks SG, Kitchen CMR, Liu L, Guo H, Gascon R, Narváez AB, Hunt P, Martin JN, Kahn JO,
644 Levy J, McGrath MS, Hecht FM. 2004. Immune activation set point during early HIV
645 infection predicts subsequent CD4+ T-cell changes independent of viral load. *Blood*
646 **104**:942–947. doi:10.1182/blood-2003-09-3333
647 Del Portillo A, Tripodi J, Najfeld V, Wodarz D, Levy DN, Chen BK. 2011. Multiploid Inheritance
648 of HIV-1 during Cell-to-Cell Infection ▿. *J Virol* **85**:7169–7176. doi:10.1128/JVI.00231-11
649 Dingens AS, Haddox HK, Overbaugh J, Bloom JD. 2017. Comprehensive mapping of HIV-1
650 escape from a broadly neutralizing antibody. *Cell Host Microbe* **21**:777-787.e4.
651 doi:10.1016/j.chom.2017.05.003
652 Doitsh G, Galloway NL, Geng X, Yang Z, Monroe KM, Zepeda O, Hunt PW, Hatano H, Sowinski
653 S, Muñoz-Arias I, Greene WC. 2014. Pyroptosis drives CD4 T-cell depletion in HIV-1
654 infection. *Nature* **505**:509–514. doi:10.1038/nature12940
655 Dufloo J, Bruel T, Schwartz O. 2018. HIV-1 cell-to-cell transmission and broadly neutralizing
656 antibodies. *Retrovirology* **15**:51. doi:10.1186/s12977-018-0434-1
657 Duncan CJA, Russell RA, Sattentau QJ. 2013. High multiplicity HIV-1 cell-to-cell transmission
658 from macrophages to CD4+ T cells limits antiretroviral efficacy. *AIDS* **27**:2201.
659 doi:10.1097/QAD.0b013e3283632ec4
660 Dupont M, Sattentau QJ. 2020. Macrophage Cell-Cell Interactions Promoting HIV-1 Infection.
661 *Viruses* **12**:492. doi:10.3390/v12050492
662 Fink SL, Cookson BT. 2005. Apoptosis, Pyroptosis, and Necrosis: Mechanistic Description of
663 Dead and Dying Eukaryotic Cells. *Infect Immun* **73**:1907–1916.
664 doi:10.1128/IAI.73.4.1907-1916.2005
665 Galloway NLK, Doitsh G, Monroe KM, Yang Z, Muñoz-Arias I, Levy DN, Greene WC. 2015.
666 Cell-to-Cell Transmission of HIV-1 Is Required to Trigger Pyroptotic Death of Lymphoid-
667 Tissue-Derived CD4 T Cells. *Cell Rep* **12**:1555–1563. doi:10.1016/j.celrep.2015.08.011
668 Giorgi JV, Hultin LE, McKeating JA, Johnson TD, Owens B, Jacobson LP, Shih R, Lewis J,
669 Wiley DJ, Phair JP, Wolinsky SM, Detels R. 1999. Shorter Survival in Advanced Human
670 Immunodeficiency Virus Type 1 Infection Is More Closely Associated with T Lymphocyte
671 Activation than with Plasma Virus Burden or Virus Chemokine Coreceptor Usage. *J*
672 *Infect Dis* **179**:859–870. doi:10.1086/314660
673 Gosselin A, Monteiro P, Chomont N, Diaz-Griffero F, Said EA, Fonseca S, Wacleche V, El-Far
674 M, Boulassel M-R, Routy J-P, Sekaly R-P, Ancuta P. 2009. Peripheral Blood
675 CCR4+CCR6+ and CXCR3+CCR6+ CD4+ T Cells Are Highly Permissive to HIV-1
676 Infection. *J Immunol* **184**:1604–1616. doi:10.4049/jimmunol.0903058
677 Gummuluru S, Rogel M, Stamatatos L, Emerman M. 2003. Binding of Human Immunodeficiency
678 Virus Type 1 to Immature Dendritic Cells Can Occur Independently of DC-SIGN and
679 Mannose Binding C-Type Lectin Receptors via a Cholesterol-Dependent Pathway. *J*
680 *Virol* **77**:12865–12874. doi:10.1128/JVI.77.23.12865-12874.2003
681 Hernandez JC, Latz E, Urcuqui-Inchima S. 2013. HIV-1 Induces the First Signal to Activate the
682 NLRP3 Inflammasome in Monocyte-Derived Macrophages. *Intervirology* **57**:36–42.
683 doi:10.1159/000353902
684 Hornung V, Ablasser A, Charrel-Dennis M, Bauernfeind F, Horvath G, Caffrey DR, Latz E,
685 Fitzgerald KA. 2009. AIM2 recognizes cytosolic dsDNA and forms a caspase-1
686 activating inflammasome with ASC. *Nature* **458**:514–518. doi:10.1038/nature07725
687 Hsiao JC, Neugroschl AR, Chui AJ, Taabazuing CY, Griswold AR, Wang Q, Huang H-C, Orth-
688 He EL, Ball DP, Hiotis G, Bachovchin DA. 2022. A ubiquitin-independent proteasome

689 pathway controls activation of the CARD8 inflammasome. *J Biol Chem* **298**:102032.
690 doi:10.1016/j.jbc.2022.102032
691 Iwami S, Takeuchi JS, Nakaoka S, Mammano F, Clavel F, Inaba H, Kobayashi T, Misawa N,
692 Aihara K, Koyanagi Y, Sato K. 2015. Cell-to-cell infection by HIV contributes over half of
693 virus infection. *eLife* **4**:e08150. doi:10.7554/eLife.08150
694 Jiang Z, Wei F, Zhang Y, Wang T, Gao W, Yu S, Sun H, Pu J, Sun Y, Wang M, Tong Q, Gao C,
695 Chang K-C, Liu J. 2021. IFI16 directly senses viral RNA and enhances RIG-I
696 transcription and activation to restrict influenza virus infection. *Nat Microbiol* **6**:932–945.
697 doi:10.1038/s41564-021-00907-x
698 Jolly C, Booth NJ, Neil SJD. 2010. Cell-Cell Spread of Human Immunodeficiency Virus Type 1
699 Overcomes Tetherin/BST-2-Mediated Restriction in T cells. *J Virol* **84**:12185–12199.
700 doi:10.1128/jvi.01447-10
701 Kulsuptrakul J, Turcotte EA, Emerman M, Mitchell PS. 2023. A human-specific motif facilitates
702 CARD8 inflammasome activation after HIV-1 infection. *eLife* **12**:e84108.
703 doi:10.7554/eLife.84108
704 Leal VNC, Reis EC, Fernandes FP, Pontillo A. 2020. NLRP3 inflammasome activation profile in
705 CD4+ T and CD19+ B lymphocytes from HIV-infected patients. *J Immunol* **204**:225.8.
706 doi:10.4049/jimmunol.204.Supp.225.8
707 Linder A, Bauernfried S, Cheng Y, Albanese M, Jung C, Keppler OT, Hornung V. 2020. CARD8
708 inflammasome activation triggers pyroptosis in human T cells. *EMBO J* **39**:e105071.
709 doi:10.15252/embj.2020105071
710 Lopez P, Koh WH, Hnatiuk R, Murooka TT. 2019. HIV Infection Stabilizes Macrophage-T Cell
711 Interactions To Promote Cell-Cell HIV Spread. *J Virol* **93**:e00805-19.
712 doi:10.1128/JVI.00805-19
713 Mamik MK, Hui E, Branton WG, McKenzie BA, Chisholm J, Cohen EA, Power C. 2017. HIV-1
714 Viral Protein R Activates NLRP3 Inflammasome in Microglia: implications for HIV-1
715 Associated Neuroinflammation. *J Neuroimmune Pharmacol* **12**:233–248.
716 doi:10.1007/s11481-016-9708-3
717 Martin N, Welsch S, Jolly C, Briggs JAG, Vaux D, Sattentau QJ. 2010. Virological Synapse-
718 Mediated Spread of Human Immunodeficiency Virus Type 1 between T Cells Is
719 Sensitive to Entry Inhibition. *J Virol* **84**:3516–3527. doi:10.1128/jvi.02651-09
720 Martínez-Méndez D, Rivera-Toledo E, Ortega E, Licona-Limón I, Huerta L. 2017. Monocyte-
721 lymphocyte fusion induced by the HIV-1 envelope generates functional heterokaryons
722 with an activated monocyte-like phenotype. *Exp Cell Res* **352**:9–19.
723 doi:10.1016/j.yexcr.2017.01.014
724 Martinez-Picado J, Savara AV, Sutton L, D'Aquila RT. 1999. Replicative fitness of protease
725 inhibitor-resistant mutants of human immunodeficiency virus type 1. *J Virol* **73**:3744–
726 3752. doi:10.1128/JVI.73.5.3744-3752.1999
727 Monroe KM, Yang Z, Johnson JR, Geng X, Doitsh G, Krogan NJ, Greene WC. 2014. IFI16 DNA
728 Sensor Is Required for Death of Lymphoid CD4 T-cells Abortively Infected with HIV.
729 *Science* **343**:428–432. doi:10.1126/science.1243640
730 Nadkarni R, Chu WC, Lee CQE, Mohamud Y, Yap L, Toh GA, Beh S, Lim R, Fan YM, Zhang
731 YL, Robinson K, Tryggvason K, Luo H, Zhong F, Ho L. 2022. Viral proteases activate the
732 CARD8 inflammasome in the human cardiovascular system. *J Exp Med* **219**:e20212117.
733 doi:10.1084/jem.20212117
734 OhAinle M, Helms L, Vermeire J, Roesch F, Humes D, Basom R, Delrow JJ, Overbaugh J,
735 Emerman M. 2018. A virus-packageable CRISPR screen identifies host factors
736 mediating interferon inhibition of HIV. *eLife* **7**:e39823. doi:10.7554/eLife.39823
737 Orenstein JM. 2000. In Vivo Cytolysis and Fusion of Human Immunodeficiency Virus Type 1-
738 Infected Lymphocytes in Lymphoid Tissue. *J Infect Dis* **182**:338–342.
739 doi:10.1086/315640

740 Peden K, Emerman M, Montagnier L. 1991. Changes in growth properties on passage in tissue
741 culture of viruses derived from infectious molecular clones of HIV-1LAI, HIV-1MAL, and
742 HIV-1ELI. *Virology* **185**:661–672. doi:10.1016/0042-6822(91)90537-L
743 Prado JG, Wrin T, Beauchaine J, Ruiz L, Petropoulos CJ, Frost SDW, Clotet B, D'Aquila RT,
744 Martinez-Picado J. 2002. Amprenavir-resistant HIV-1 exhibits lopinavir cross-resistance
745 and reduced replication capacity. *AIDS Lond Engl* **16**:1009–1017.
746 doi:10.1097/00002030-200205030-00007
747 Primiano MJ, Lefker BA, Bowman MR, Bree AG, Hubeau C, Bonin PD, Mangan M, Dower K,
748 Monks BG, Cushing L, Wang S, Guzova J, Jiao A, Lin L-L, Latz E, Hepworth D, Hall JP.
749 2016. Efficacy and Pharmacology of the NLRP3 Inflammasome Inhibitor CP-456,773
750 (CRID3) in Murine Models of Dermal and Pulmonary Inflammation. *J Immunol*
751 **197**:2421–2433. doi:10.4049/jimmunol.1600035
752 Resch W, Ziermann R, Parkin N, Gamarnik A, Swanstrom R. 2002. Nelfinavir-resistant,
753 amprenavir-hypersusceptible strains of human immunodeficiency virus type 1 carrying
754 an N88S mutation in protease have reduced infectivity, reduced replication capacity, and
755 reduced fitness and process the Gag polyprotein precursor aberrantly. *J Virol* **76**:8659–
756 8666. doi:10.1128/jvi.76.17.8659-8666.2002
757 Richardson MW, Carroll RG, Stremlau M, Korokhov N, Humeau LM, Silvestri G, Sodroski J,
758 Riley JL. 2008. Mode of Transmission Affects the Sensitivity of Human
759 Immunodeficiency Virus Type 1 to Restriction by Rhesus TRIM5α. *J Virol* **82**:11117–
760 11128. doi:10.1128/jvi.01046-08
761 Rodriguez-Garcia M, Barr FD, Crist SG, Fahey JV, Wira CR. 2014. Phenotype and susceptibility
762 to HIV infection of CD4+ Th17 cells in the human female reproductive tract. *Mucosal*
763 *Immunol* **7**:1375–1385. doi:10.1038/mi.2014.26
764 Roesch F, OhAinle M, Emerman M. 2018. A CRISPR screen for factors regulating SAMHD1
765 degradation identifies IFITMs as potent inhibitors of lentiviral particle delivery.
766 *Retrovirology* **15**:26. doi:10.1186/s12977-018-0409-2
767 Russell RA, Martin N, Mitar I, Jones E, Sattentau QJ. 2013. Multiple proviral integration events
768 after virological synapse-mediated HIV-1 spread. *Virology* **443**:143–149.
769 doi:10.1016/j.virol.2013.05.005
770 Stanford - HIV Drug Resistance Database. n.d. https://hivdb.stanford.edu/page/release-
771 notes/#consensusbsequences
772 Thompson MR, Sharma S, Atianand M, Jensen SB, Carpenter S, Knipe DM, Fitzgerald KA,
773 Kurt-Jones EA. 2014. Interferon γ-inducible Protein (IFI) 16 Transcriptionally Regulates
774 Type I Interferons and Other Interferon-stimulated Genes and Controls the Interferon
775 Response to both DNA and RNA Viruses. *J Biol Chem* **289**:23568–23581.
776 doi:10.1074/jbc.M114.554147
777 Toohey K, Wehrly K, Nishio J, Perryman S, Chesebro B. 1995. Human immunodeficiency virus
778 envelope V1 and V2 regions influence replication efficiency in macrophages by affecting
779 virus spread. *Virology* **213**:70–79. doi:10.1006/viro.1995.1547
780 Tsu BV, Agarwal R, Gokhale NS, Kulsuptrakul J, Ryan AP, Fay EJ, Castro LK, Beierschmitt C,
781 Yap C, Turcotte EA, Delgado-Rodriguez SE, Vance RE, Hyde JL, Savan R, Mitchell PS,
782 Daugherty MD. 2023. Host-specific sensing of coronaviruses and picornaviruses by the
783 CARD8 inflammasome. *PLOS Biol* **21**:e3002144. doi:10.1371/journal.pbio.3002144
784 Varghese V, Mitsuya Y, Fessel WJ, Liu TF, Melikian GL, Katzenstein DA, Schiffer CA, Holmes
785 SP, Shafer RW. 2013. Prototypical Recombinant Multi-Protease-Inhibitor-Resistant
786 Infectious Molecular Clones of Human Immunodeficiency Virus Type 1. *Antimicrob*
787 *Agents Chemother* **57**:4290–4299. doi:10.1128/AAC.00614-13
788 Vermeire J, Naessens E, Vanderstraeten H, Landi A, Iannucci V, Van Nuffel A, Taghon T,
789 Pizzato M, Verhasselt B. 2012. Quantification of reverse transcriptase activity by real-

790 time PCR as a fast and accurate method for titration of HIV, lenti- and retroviral vectors.
791 *PloS One* **7**:e50859. doi:10.1371/journal.pone.0050859
792 Walter BL, Wehrly K, Swanstrom R, Platt E, Kabat D, Chesebro B. 2005. Role of low CD4 levels
793 in the influence of human immunodeficiency virus type 1 envelope V1 and V2 regions on
794 entry and spread in macrophages. *J Virol* **79**:4828–4837. doi:10.1128/JVI.79.8.4828-
795 4837.2005
796 Wang Q, Clark KM, Tiwari R, Raju N, Tharp GK, Rogers J, Harris RA, Raveendran M, Bosinger
797 SE, Burdo TH, Silvestri G, Shan L. 2024. The CARD8 inflammasome dictates HIV/SIV
798 pathogenesis and disease progression. *Cell* **187**:1223-1237.e16.
799 doi:10.1016/j.cell.2024.01.048
800 Wang Q, Gao H, Clark KM, Mugisha CS, Davis K, Tang JP, Harlan GH, DeSelm CJ, Presti RM,
801 Kutluay SB, Shan L. 2021. CARD8 is an inflammasome sensor for HIV-1 protease
802 activity. *Science* **371**:eabe1707. doi:10.1126/science.abe1707
803 Wannamaker W, Davies R, Namchuk M, Pollard J, Ford P, Ku G, Decker C, Charifson P, Weber
804 P, Germann UA, Kuida K, Randle JCR. 2007. (S)-1-((S)-2-{[1-(4-amino-3-chloro-phenyl)-
805 methanoyl]-amino}-3,3-dimethyl-butanoyl)-pyrrolidine-2-carboxylic acid ((2R,3S)-2-
806 ethoxy-5-oxo-tetrahydro-furan-3-yl)-amide (VX-765), an orally available selective
807 interleukin (IL)-converting enzyme/caspase-1 inhibitor, exhibits potent anti-inflammatory
808 activities by inhibiting the release of IL-1beta and IL-18. *J Pharmacol Exp Ther* **321**:509–
809 516. doi:10.1124/jpet.106.111344
810 Xie M, Leroy H, Mascarau R, Woottum M, Dupont M, Ciccone C, Schmitt A, Raynaud-Messina
811 B, Vérollet C, Bouchet J, Bracq L, Benichou S. 2019. Cell-to-Cell Spreading of HIV-1 in
812 Myeloid Target Cells Escapes SAMHD1 Restriction. *mBio* **10**:10.1128/mbio.02457-19.
813 doi:10.1128/mbio.02457-19
814 Zhang C, Song J-W, Huang H-H, Fan X, Huang L, Deng J-N, Tu B, Wang K, Li J, Zhou M-J,
815 Yang C-X, Zhao Q-W, Yang T, Wang L-F, Zhang J-Y, Xu R-N, Jiao Y-M, Shi M, Shao F,
816 Sékaly R-P, Wang F-S. 2021. NLRP3 inflammasome induces $CD4^+$ T cell loss in
817 chronically HIV-1–infected patients. *J Clin Invest* **131**. doi:10.1172/JCI138861
818 Zhong P, Agosto LM, Ilinskaya A, Dorjbal B, Truong R, Derse D, Uchil PD, Heidecker G, Mothes
819 W. 2013. Cell-to-Cell Transmission Can Overcome Multiple Donor and Target Cell
820 Barriers Imposed on Cell-Free HIV. *PLOS ONE* **8**:e53138.
821 doi:10.1371/journal.pone.0053138
822
823

824 **Supplemental Note**

825

826 There have been 4 different sublines of THP-1 cells previously characterized (Kasai et
827 al., 2022). Using short tandem repeat (STR) profiling, we were able to distinguish the WT THP-1
828 cell stocks that were used as the parental line for knockouts and complemented knockouts in
829 this work and our prior work (Kulsuptrakul et al., 2023), as distinct from WT THP-1 cells sourced
830 from ATCC at 3 different loci (**Figure A1A**). Of note, unlike the THP-1 cells used here (referred
831 to as JK THP-1), ATCC THP-1 cells elicited IL-1β secretion in the absence of HIV-1 infection in
832 the presence of 20μg/mL DEAE-dextran (**Figure A1B**). Unless otherwise specified, any mention
833 of "THP-1 cells" are referring to our JK THP-1 cells, not ATCC THP-1 cells. Nonetheless, given
834 the sensitivity of some THP-1 sublines to elicit an inflammasome response in the presence of
835 DEAE-dextran, we assessed whether or not we could establish systems to measure HIV-1
836 induced CARD8-dependent inflammasome activation in the absence of DEAE-dextran. Thus,
837 we infected either wildtype (WT) or *CARD8* knockout (KO) THP-1 cells with wildtype HIV-1_{LAI} in
838 either the presence or absence of DEAE-dextran and measured cell death and IL-1β secretion
839 24 hours post-infection as readouts of inflammasome activation. We found that despite
840 achieving similar levels of infection (20-30%) as measured by intracellular $p24^{gag}$ after
841 spinoculation with and without DEAE-dextran (**Figure A1C,** left), we detected robust CARD8-
842 dependent inflammasome activation in WT THP-1 cells infected only in the presence of DEAE-
843 dextran (**Figure A1C,** middle and right). These data suggest that cationic polymer is necessary
844 to observe HIV-dependent CARD8 inflammasome activation in our cell-free system.

A

Cell Line:	JK THP-1		ATCC THP-1	
Expasy Best Match Cell Line No:	CVCL_5115		CVCL_E2QQ	
Marker	**Allele 1**	**Allele 2**	**Allele 1**	**Allele 2**
AMEL	X	Y	X	Y
D3S1358	15	17	15	17
D1S1656	16	17	16	17
D2S441	10	11	10	11
D10S1248	14		14	
D13S317	8	13	13	
Penta E	11	15	11	15
D16S539	11	12	11	12
D18S51	13	14	13	14
D2S1338	17	18	17	18
CSF1PO	11	13	11	13
Penta D	10	12	10	12
TH01	8	9.3	8	9.3
vWA	16	17	16	
D21S11	30	31.2	30	31.2
D7S820	10		10	
D5S818	11	12	11	12
TPOX	8	11	8	11
DYS391	10		10	
D8S1179	10	14	10	14
D12S391	18	19	19	
D19S433	12.2	13	12.2	13
FGA	24	25	24	25
D22S1045	11	15	11	15

B

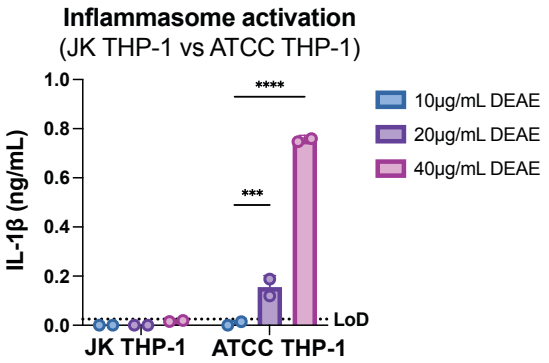

C

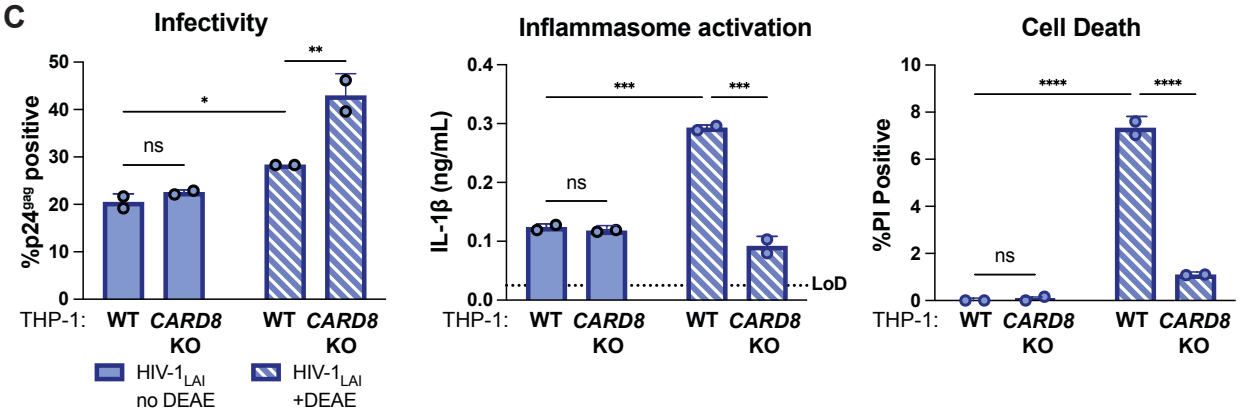

Figure A1. Characterization of THP-1 cells. (A) Promega GenePrint® 24 system STR analysis summary of our JK THP-1 cells versus ATCC THP-1 cells. Cell line authentication was done by TransnetYX, Inc. by following the protocol described in ANSI/ATCC ASN-0002-2011. The STR alleles were searched on the ATCC Database and the Expasy best match cell numbers for each cell line had a 100% database match. Distinguishing loci are highlighted in yellow and distinguishing alleles are in red. **(B)** JK and ATCC THP-1 cells were primed with Pam3CSK4 overnight then treated with increasing doses of DEAE-dextran for 24 hours before probing for IL-1β secretion. (**C**) Wildtype (WT) or *CARD8* knockout (KO) THP-1 cells were infected with wildtype HIV-1_{LAI} at the same MOI in the presence or absence of DEAE-dextran (10μg/mL) then harvested after 24 hours and assayed for: left) percent infection via intracellular $p24^{gag}$, middle) inflammasome activation by IL-1β secretion via IL-1R reporter assay, and right) cell death via propidium iodide (PI) dye uptake using flow cytometry. %PI positive and IL-1 levels are normalized to mock control. Dotted line indicates limit of detection (LoD). Datasets represent mean ± SD (n=2 biological replicates). Two-way ANOVA with (B) Sidak's or (C) Tukey's test using GraphPad Prism 10. ns = not significant, *p<0.05,**p<0.01, ***p<0.001, ****p<0.0001.

861 **Supplemental Note References**
862
863 Kasai F, Hirayama N, Fukushima M, Kohara A, Nakamura Y. 2022. THP-1 reference data:
864 Proposal of an in vitro branched evolution model for cancer cell lines. *Int J Cancer*
865 **151**:463–472. doi:10.1002/ijc.34019
866 Kulsuptrakul J, Turcotte EA, Emerman M, Mitchell PS. 2023. A human-specific motif facilitates
867 CARD8 inflammasome activation after HIV-1 infection. *eLife* **12**:e84108.
868 doi:10.7554/eLife.84108
869